

Seminar series nr 172

# Relating interannual variability of atmospheric CH<sub>4</sub> growth rate to large-scale CH<sub>4</sub> emissions from northern wetlands

Sophie Rychlik

---

2009  
Geobiosphere Science Centre  
Physical Geography and Ecosystems Analysis  
Lund University  
Sölvegatan 12  
S-223 62 Lund  
Sweden





Relating interannual variability of atmospheric CH<sub>4</sub>  
growth rate to large-scale CH<sub>4</sub> emissions from  
northern wetlands

Sophie Rychlik

Master Degree thesis in  
Physical Geography and Ecosystem Analysis

*Supervisor:*

Torben R. Christensen

Department of  
Physical Geography and Ecosystem Analysis  
Lund University 2009 Nr. 172



## Abstract

The increasing atmospheric concentration of the greenhouse gas methane (CH<sub>4</sub>) is highly relevant for current and future global warming. Since the mid-1980s atmospheric measurements have revealed large interannual fluctuations in methane growth rate. However, the causes of this feature are still not well understood. In 2007, a peak in growth rate appears to have been particularly strong at high northern latitudes.

Apart from anthropogenic emissions, natural wetlands are globally the single largest source of atmospheric CH<sub>4</sub>. Studies at multiple northern wetland sites have shown that soil temperature is a dominant controlling factor of wetland emissions. It has been suggested that strong anomalous warming could cause an increase in wetland CH<sub>4</sub> emissions, and that northern wetlands may be a major contributor to the observed atmospheric growth rate variability.

This study is concerned with investigating a potential relation between interannual variations in atmospheric CH<sub>4</sub> growth rate and that of accumulated large-scale emission anomalies from northern wetlands. With wetland distribution data for the circumpolar north between 53°N-90°N, emissions are estimated as a function of soil temperature anomaly. Special attention is given to the 2007 growth rate event, but the interannual variation of anomalous warming and estimated emissions are also considered for the time period 1992-2008.

It is found that a relation does exist. When a time series of estimated July (peak season) CH<sub>4</sub> emissions is considered separately the correlation with interannual growth rate variability becomes more apparent, and 2007 stands out with a pronounced emission peak. The results suggest that the impact of anomalous soil temperatures on peak season emissions is particularly important, and that it may further have an influence on late season emissions. Discrepancies between the atmospheric and emission time series also suggest that, in some years, the impact of other environmental factors and emission sources (e.g. forest fires) may limit the relevance of northern wetlands.

In general, the estimated CH<sub>4</sub> emission values do not fully correspond to the CH<sub>4</sub> amount required (estimated) to explain the growth rate anomalies. However, due to uncertainties in the emission estimation method, we have more confidence in the significance of the found relation between relative interannual variations from 1992 to 2008. It is concluded that this study strongly points at northern wetlands being a key emission source in terms of atmospheric CH<sub>4</sub> growth rate variability in high northern latitudes, and perhaps also globally.

**Keywords:** Physical Geography, northern wetlands, CH<sub>4</sub>, emission sources, temperature sensitivity, interannual variability, atmospheric growth rate, July

Supervisor: Torben R. Christensen  
Master Degree thesis in Physical Geography and Ecosystem Analysis. Autumn 2009. Seminar series nr 172  
Department of Physical Geography and Ecosystem Analysis, Lund University.

## Sammanfattning

Metan (CH<sub>4</sub>) är en av de viktigaste växthusgaserna i atmosfären och dess kraftiga ökning har bidragit till den uppvärmning som vi har upplevt fram till idag. Sedan mitten av 1980-talet påvisar mätningar att metantillväxten i atmosfären har börjat fluktuera från år till år. Orsakerna till detta är omstridda och ännu inte klargjorda. Under 2007 uppmättes en kraftig ökning i tillväxt som var särskilt markant på högt nordliga breddgrader.

Bortsett från antropogena utsläpp, är naturliga våtmarker på global skala den enskilt största emissionskällan av metan. Upprepade mätningar på ett flertal nordliga våtmarker visar att marktemperatur är en viktig kontrollerande faktor för metanproduktion och utsläpp. Höga temperaturanomalier tros därför kunna orsaka en ökning av metanutsläpp från våtmarker.

Denna studie undersöker om det finns ett samband mellan variationer i årlig tillväxt av metan i atmosfären och storskaliga metanutsläpp från nordliga våtmarker. Data över utbredningen av våtmarker används för att estimerar utsläpp som funktion av marktemperaturanomali. Särskild fokus läggs på tillväxttoppen som uppmärksammades 2007, men även mellanårsvariationen av temperaturanomali och de uppskattade metanutsläppen analyseras för tidsperioden 1992-2008.

Resultaten visar på att ett samband existerar. Då en tidsserie av uppskattade metanutsläpp från juli månad analyseras separat blir korrelationen till mellanårsvariationen av tillväxt tydligare, och 2007 utmärker sig med en markant emissionstopp. Detta tyder på att förhöjda marktemperaturer under växtsäsongens mitt har särskilt stor betydelse, och att de eventuellt också kan ha inverkan på utsläpp som sker senare på hösten. Avvikelser mellan tidsserierna av atmosfärstillväxt och de beräknade metanemissionerna tyder också på att det, under vissa år, finns andra miljöfaktorer och emissionskällor (t.ex. skogsbränder) som begränsar betydelsen av nordliga våtmarker.

Generellt uppnår inte de uppskattade emissionsvärdena de mängder CH<sub>4</sub> som krävs (uppskattas) för att förklara individuella avvikelser i årlig metantillväxt i atmosfären. Men eftersom det finns flera osäkerheter i uppskattningsmetoden, anses det funna sambandet mellan relativ mellanårsvariation ändå tala för att nordliga våtmarker har en nyckelroll i förklaringen till de årliga fluktuationerna av metantillväxt i atmosfären på högt nordliga breddgrader, och kanske även globalt.

**Nyckelord:** Naturgeografi, nordliga våtmarker, metan, emissionskällor, temperaturkänslighet, mellanårsvariation, atmosfärisk tillväxt, juli

Handledare: Torben R. Christensen

Masterexamensuppsats i Naturgeografi och Ekosystemanalys. Höst 2009. Seminarieuppsatser nr 172  
Institutionen för Naturgeografi och Ekosystemanalys, Lunds Universitet.

## TABLE OF CONTENTS

---

Abstract .....	5
Sammanfattning .....	6
1. INTRODUCTION.....	9
1.1 Objectives and Hypothesis.....	9
2. BACKGROUND.....	11
2.1 The global methane budget.....	11
2.2 Variations in annual atmospheric CH <sub>4</sub> growth rate.....	12
2.3 Possible explanations for CH <sub>4</sub> growth rate variability .....	13
2.4 Estimating methane source emissions.....	14
2.4.1 <i>Different approaches</i> .....	14
2.4.2 <i>Soil temperature as a control of CH<sub>4</sub> flux from northern wetlands</i> .....	15
3. METHOD.....	19
3.1 Overview .....	19
3.2 Data .....	21
3.3 Wetland area and temperature anomalies .....	22
3.4 Estimating CH <sub>4</sub> emissions.....	23
3.4.1 <i>Finding the anomaly impact - first approach</i> .....	23
3.4.2 <i>Finding the anomaly impact - second approach</i> .....	24
3.5 Comparing estimated emissions with atmospheric data .....	24
3.6 Evaluating the CH <sub>4</sub> emission computation model.....	25
4. RESULTS.....	27
4.1 The strength and distribution of temperature anomalies.....	27
4.2 Estimated CH <sub>4</sub> emission anomalies and atmospheric growth rate for 2007 .....	29
4.3 Comparing relative interannual variation, 1992-2008 .....	32
4.4 Evaluation of the CH <sub>4</sub> emission computation model .....	36
5. DISCUSSION .....	39
5.1 Evaluation of uncertainties in the method .....	39
5.2 Comparing estimated CH <sub>4</sub> emission anomalies with atmospheric growth rate .....	40
6. CONCLUSIONS .....	43
<i>Acknowledgements</i> .....	45
<i>Cited references</i> .....	46
<i>Web sources</i> .....	48
APPENDIX.....	49



# 1. INTRODUCTION

---

Methane (CH<sub>4</sub>) is an important greenhouse gas that is beginning to take more place in the overall debate on global warming, as well as in scientific research. In the most recent report from the Intergovernmental Panel on Climate Change (IPCC, 2007), the projected role of methane for future global warming received a lot of attention due to new features in the trend of global CH<sub>4</sub> concentrations in the atmosphere. While the overall increasing trend appears to be declining, since the mid-1980s, unprecedented large fluctuations in annual growth rate puzzle the research community. Finding the causes of this new feature is a pressing issue that is still not well resolved. However, it is likely that changes are occurring in the imbalance between CH<sub>4</sub> emission sources and sinks, where the relative strength of different sources may have shifted (Dlugokencky *et al.*, 1998; IPCC, 2007).

A large portion of global CH<sub>4</sub> emissions is produced through microbial decomposition, a biological process that is largely influenced by climatic variables such as moisture and temperature (IPCC, 2007). In a modelling study by Dlugokencky *et al.* (2001), a clear link between CH<sub>4</sub> emissions from wetlands and climate was confirmed. This makes the interannual variation of the wetland source, which is furthermore the single largest global emission source, highly relevant. Wetland ecosystems cover extensive areas in arctic and subarctic regions, which are currently experiencing substantial warming. Consequently, northern wetlands are one of the primary emission sources that have been suggested contribute to a large part of the observed interannual variation in atmospheric CH<sub>4</sub> growth rate (Bousquet *et al.*, 2006; Dlugokencky *et al.*, 2001).

## 1.2 Objectives and Hypothesis

The main purpose of this study is to contribute to a better understanding of the relation between CH<sub>4</sub> emissions from northern high latitude wetlands and variations in annual atmospheric CH<sub>4</sub> growth rate. The most recent major growth rate peak occurred in 2007 (Rigby *et al.*, 2008; web source [2]). This event is particularly interesting due to other coinciding circumstances, one of them being the extensive melting of the arctic ice-sheet between 2006 and 2007 (web source [1]), which suggests high temperature anomalies occurring over high northern latitudes. Furthermore, for the same year, Mastepanov *et al.* (2008) present the discovery of a large burst of late season CH<sub>4</sub> emissions at an arctic wetland measurement site on Greenland. This was observed at the onset of soil freezing, when CH<sub>4</sub> flux rates are otherwise expected to be very low. Although this phenomenon may not be connected to the atmospheric growth rate peak in question, it reinforces the relevance of studying the contribution CH<sub>4</sub> emissions from arctic wetland ecosystems.

Studies have shown that soil temperature is an important environmental factor that controls the magnitude of CH<sub>4</sub> emissions from wetlands (e.g. Christensen *et al.*, 2003; Jackowicz-Korczyński *et al.*, *submitted*). In this study such a temperature dependency lies as a foundation for the hypothesis that *variations in annual wetland CH<sub>4</sub> emissions can (to some extent) explain the interannual variability of atmospheric CH<sub>4</sub> growth rate*. The main objective of the study is to apply the stated hypothesis for the time period 1992-2008 in order to explore the following questions:

- Can wetland methane emissions explain the 2007 CH<sub>4</sub> growth rate peak in high northern latitudes?
- Is there a relation between the magnitude of anomalous warming and atmospheric CH<sub>4</sub> growth rate in high northern latitudes?
- Is there a relation between interannual variation of anomalous wetland CH<sub>4</sub> emissions and atmospheric CH<sub>4</sub> growth rate in high northern latitudes?

## 2. BACKGROUND

### 2.1 The global methane budget

The sources of atmospheric methane are commonly divided into two groups – *anthropogenic* and *natural*. Wetland emissions are among the natural sources along with oceans, forests, fire, termites and geological sources. Anthropogenic sources, the direct result of human activity, include fossil fuel combustion, biomass burning, landfills and waste treatment, rice agriculture, and livestock (IPCC, 2007). Figure 2.1 illustrates an approximation of the relative contribution of the different sources. The human induced emissions stand for a larger part of the total global emission, but about 70% of all natural emissions originate from wetland ecosystems, such as marshes, swamps, bogs, and peatlands in the tropics and the high northern latitudes (Chapin III, Matson, and Mooney, 2002).

Observe that although wild fire does not exist as a separate source sector in Figure 2.1, within the topic of CH<sub>4</sub> growth rate variability, in current literature it is considered being a potentially important source contributor (see Section 2.3). Since the extent of fire may vary substantially from year to year, depending on heat and drought conditions, this seems logical. Furthermore, there exists a somewhat confusing inconsistency in the literature, where wild fire, a natural source, is sometimes also referred to as *biomass burning*. This is however generally categorized as an anthropogenic source.

Methane is produced under anaerobic conditions (i.e. no oxygen is available), and in wetland ecosystems this occurs as a biological process where organic material is decomposed by so called methanogenic bacteria. In this case, methane is said to be of *biogenic* origin.

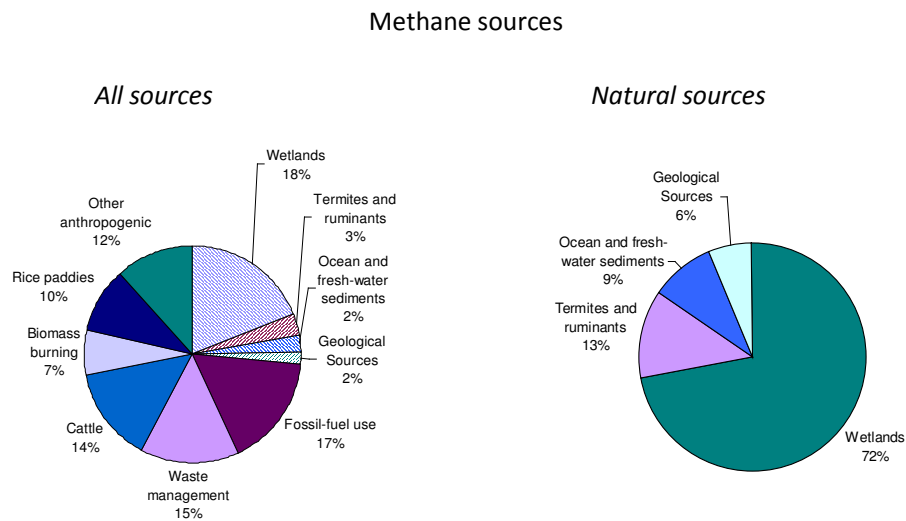


**Figure 2.1** An approximation of relative emission contribution from different CH<sub>4</sub> sources as taken from Schlesinger (1997) cited in Chapin III, Matson, and Mooney (2002). In the left chart, the sectors with striped structure belong to the category of *natural emission sources*. In the right chart, it is clear to see that wetlands are the dominating source of natural CH<sub>4</sub> emissions.

Once in the atmosphere, CH<sub>4</sub> is readily removed (oxidized) by the hydroxyl free radical (OH), and this process stands for about 90% of the total global methane sink. Two other minor sinks are destruction in the stratosphere, and oxidation in soils. CH<sub>4</sub> is removed faster from the atmosphere than for example carbondioxide (CO<sub>2</sub>). The average lifetime of CH<sub>4</sub> is about  $8.7 \pm 1.3$  years and the current global average atmospheric concentration is about 1,774 ppb (IPCC, 2007). Since measurements were initiated in the middle of the 20<sup>th</sup> century the concentration of atmospheric CH<sub>4</sub> has been steadily increasing. This is the result of an imbalance between the size of the global emission source and the global methane sink. The amount of emitted CH<sub>4</sub> overwhelms the atmosphere's capacity to remove CH<sub>4</sub>, causing an increase in the methane load and concentration. This trend is commonly described in terms of atmospheric *growth rate*, meaning the average change in atmospheric CH<sub>4</sub> burden over a year, expressed in Tg (CH<sub>4</sub>) yr<sup>-1</sup> or ppb yr<sup>-1</sup>.

## 2.2 Variations in annual atmospheric CH<sub>4</sub> growth rate

In the late 1970s and early 1980s the CH<sub>4</sub> growth rate averaged around 14 ppb yr<sup>-1</sup> (~1% increase per year) (Blake and Rowland, 1988), but since the mid-1980s a new *declining* trend in growth rate has been observed (Dlugokencky *et al.*, 2003). In connection with the overall declining trend, there has furthermore occurred a substantial variation in growth rate from one year to the next. From 1992 to 2008, this interannual variability is demonstrated by a series of growth rate peaks occurring in 1993-1994, 1998, 2002-2003 (Dlugokencky *et al.*, 2003), and most recently in 2007 (web source [2]; Rigby *et al.*, 2008). Low growth rate events were observed in 1992 and 2004. The variation can be viewed in Figure 2.2 below.

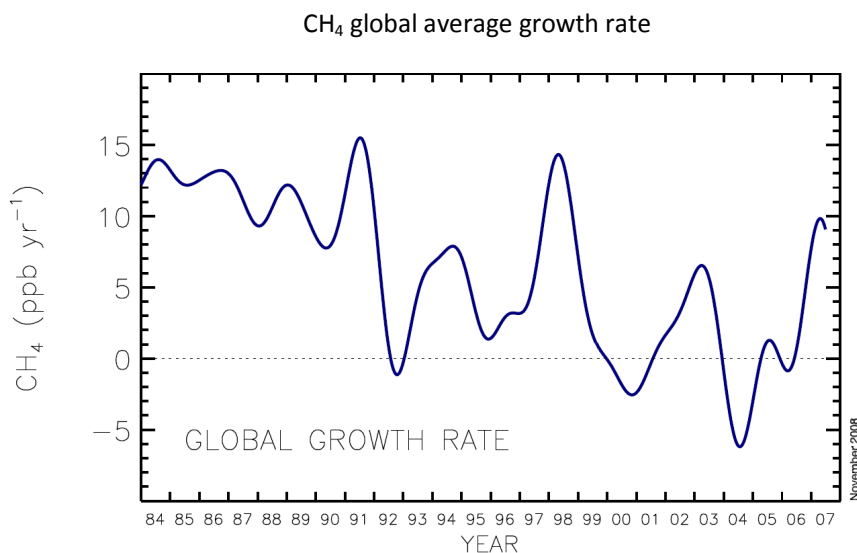


**Figure 2.2** The graph shows the development of global average CH<sub>4</sub> growth rate over time as derived from the NOAA/GMD network of surface air sampling sites. There is a clear decreasing trend, and since 1990 there is significant interannual variability. [Borrowed from NOAA/ESRL Carbon Cycle, Boulder, Colorado. Dr. Ed Dlugokencky, <http://www.esrl.noaa.gov/gmd/ccgg/>]

In general, the magnitude of the *total* global CH<sub>4</sub> source is quite well known, but in terms of the strength of *individual* sources and their trend over time, a lot of uncertainty remains (Dlugokencky *et al.*, 1998; IPCC, 2007). Therefore, at present time there are still no definite and consistent explanations for the variability, and the implication it might have for the future, primarily in terms of climate change. The anomalous growth rate events have been used to test the current understanding of how different emission sources may have contributed to the interannual variation (Dlugokencky *et al.*, 2003). And this is also how the contribution of wetland CH<sub>4</sub> emissions will be evaluated in the current study.

### 2.3 Possible explanations for CH<sub>4</sub> growth rate variability

There is a range of suggested hypotheses regarding the causes of recent interannual variation in CH<sub>4</sub> growth rate. In simple terms, the variation may either be the result of anomalous emissions from one or several sources, or a variation in the removal rate of methane in the atmosphere. Both the sources and the atmospheric sink are in turn dependent on human activity, climatic factors, and atmospheric transport.

As mentioned earlier, the atmospheric CH<sub>4</sub> sink is controlled by the abundance of the hydroxyl free radical (OH) in the atmosphere, which is in turn sensitive to different components of the atmospheric system. According to the IPCC (2007) it is likely that interannual variation in OH has an impact on CH<sub>4</sub> growth rate. However, it is difficult to measure and model OH levels and trends over time, and in general there appears to still exist significant uncertainties related to this important sink component.

For the purpose of this study, the role of the CH<sub>4</sub> sink will not be mentioned in further detail. Instead, focus lies on the contribution of emissions from *northern wetlands* and *boreal fires* (burning) – two natural sources that are often discussed in the scientific literature. In an initial analysis of atmospheric measurement data from 2007, Rigby *et al.* (2008) mention that an increase in a natural emission source (e.g. boreal and tropical wetlands and biomass burning) is the most probable explanation for the 2007 CH<sub>4</sub> growth rate peak since such a sudden change in anthropogenic emissions is unlikely. The peak is furthermore found to likely being more pronounced in the Northern Hemisphere, which puts light on the observed high anomalous warming occurring over Siberia, where extensive wetlands are found (Rigby *et al.*, 2008). This could be an indication of anomalous high CH<sub>4</sub> emissions from wetlands in the region.

Also, in a recent top-down modelling study (see next section for a basic description of modelling approaches), wetlands were suggested the dominant source responsible for interannual variations in methane emissions for the period 1984-2003, followed by fire emissions (Bousquet *et al.*, 2006). This conclusion supports an earlier study, Dlugokencky *et al.* (2001), which attributed the 1998 large growth rate event primarily to wetland emissions, and to a lesser extent, to *boreal biomass burning* (forest fires). Using a global process-based model (with temperature and precipitation anomaly as input), the authors emphasise that in terms of spatial and seasonal pattern the estimated wetland CH<sub>4</sub> emission anomalies correspond well with the spatial and seasonal atmospheric observations of growth rate, which strengthens the wetland source hypothesis.

However, 1998 was a strong El Niño year causing warm temperature and precipitation anomalies globally as well as in the arctic and subarctic regions (IPCC, 2007). The occurrence of widespread dryness causing extensive wild forest fires and CH<sub>4</sub> emissions is therefore more frequently suggested as the main explanation for the high atmospheric growth rate in 1998 (Bousquet *et al.*, 2006, Langenfelds *et al.*, 2002; Van der Welf *et al.*, 2004). In Simmonds *et al.* (2005), boreal fires is also strongly argued the cause for the smaller 2002-2003 growth rate increase.

During the event of biomass burning, besides CH<sub>4</sub> (and of course CO<sub>2</sub>), the gas *carbonmonoxide* (CO) is also produced. Increases in boreal fire have been found to influence atmospheric CO (Kasischke *et al.*, 2005). Therefore, when a CH<sub>4</sub> growth rate event is paralleled by an increase in CO growth rate, it points at fires being the main source contributing to the CH<sub>4</sub> increase (Rigby *et al.*, 2008). However, in the case of 2007, Rigby *et al.* (2008) highlight that the large CH<sub>4</sub> increase in the Northern Hemisphere was *not* accompanied by a peak in CO growth rate. This is confirmed by atmospheric data by NOAA/GMD (web source [2]), and reinforces anomalous high emissions from wetlands, particularly *northern wetlands*, as being the main cause for the 2007 CH<sub>4</sub> growth rate increase.

In case of the 1992 growth rate decrease, many studies refer to the volcanic eruption of Mt. Pinatubo (in the Philippines) in 1991 to explain the event. Northern wetlands are also present in this discussion, since cold temperatures due to a darkening effect of volcanic aerosols in the atmosphere may have caused a decrease in wetland emission in northern latitudes (Hogan and Harriss, 1994). Another suggestion is that a major decrease in fossil fuel combustion due to the economic collapse of the former Soviet Union caused a general growth rate decrease in the early 1990s (Law and Nisbet, 1996; Dlugokencky *et al.*, 1998).

## 2.4 Estimating methane source emissions

### 2.4.1 Different approaches

Among the above mentioned studies and others, different approaches are used to estimate CH<sub>4</sub> emission rates and the relative contribution of different sources. Often this is done by the help of computer models. Emissions can either be estimated “from the ground” (bottom-up approach) using process-based models, or they can be estimated from atmospheric measurement data through inverse-modelling (top-down approach).

In the case of wetland CH<sub>4</sub> emissions, in the first modelling approach, process-based models are used to quantify methane production by applying current knowledge of the relation between environmental factors and conditions, climate, and gas flux. This is however quite difficult to do (especially on a large-scale) because of the complex dynamics of gas production and exchange between the ground and atmosphere. In general, bottom-up estimations tend to underestimate wetland emissions compared to top-down estimations (Christensen *et al.*, 1996).

The second approach requires continuous (in time) observations of atmospheric concentrations, optimally from well-distributed global measurement networks (IPCC, 2007). Examples of existing networks are AGAGE and NOAA/CMDL. The inverse models are employed

to try to “track” the spatial source of emissions on the ground. In other words, atmospheric CH<sub>4</sub> is linked to emissions from geographical locations, but the actual source type remains unknown. In combination with this top-down approach, some studies attempt to further specify the exact source by analysis of (molecular) isotope composition. The isotope signature, or the <sup>13</sup>C/<sup>12</sup>C ratio of methane, differs depending on the production process, for example if it is of biogenetic (from microbial production) or non-biogenetic origin (e.g. from fossil fuel combustion) (Mikaloff Fletcher *et al.*, 2004).

A third and more empirical approach is to use CH<sub>4</sub>-flux rate measurements from specific sites and extrapolate them to obtain large-scale emission estimations. This approach will be used here. More exactly, we will use an empirical relationship between soil temperature and CH<sub>4</sub> flux from a single site and extrapolate it over the Northern Hemisphere. This will be described in more detail in the Method section.

#### 2.4.2 Soil temperature as a control of CH<sub>4</sub> flux from northern wetlands

The processes and environmental controls involved in the production of CH<sub>4</sub>, and release from wetlands, are numerous and complex. In this study, focus lies on the controlling factor *soil temperature*, on which microbial production of methane is known to be strongly dependent. In recent findings, the correlation between soil temperature and CH<sub>4</sub> flux rates have been reinforced, both in terms of large-scale variations (Christensen *et al.*, 2003) and local-scale variations (Jackowicz-Korczyński *et al.*, *submitted*).

Christensen *et al.* (2003) compared CH<sub>4</sub> flux measurements from five different northern wetland sites located in varying climatic zones. The most southern site is found in continental temperate Siberia (Russia) at 57°01'N, and the most northern site is located in high arctic Greenland at 74°30'N. The study found a strong (exponential) correlation between mean seasonal soil temperature and mean seasonal CH<sub>4</sub> flux, which suggests that soil temperature is a good predictor for large-scale and interannual variations in CH<sub>4</sub> emissions (Christensen *et al.*, 2003).

There are also other local environmental factors that have been related to CH<sub>4</sub> flux rates. Two very important factors are substrate (organic material available for decomposition) (Christensen *et al.*, 2003), and soil moisture or water table height (e.g. Waddington *et al.*, 1996; MacDonald *et al.*, 1998). However, according to Christensen *et al.* (2003), under the conditions of relatively high water table levels, there is no apparent relation between small variations in water table position and CH<sub>4</sub> flux. Instead it is suggested, that in terms of large-scale variations, the water table functions as an “on-off switch” for high CH<sub>4</sub>-emitting northern wetlands. When the water table falls below a threshold level, it becomes a strong limiting factor for CH<sub>4</sub> flux, and as a result, emissions drop drastically (Christensen *et al.*, 2003).

The above described study and results are based on weekly or biweekly flux measurements performed during the growing season over a total of 12 years. Consequently, the derived correlation is based on *seasonal means*. In the present study we will therefore use another, however similar, exponential relationship between soil temperature and CH<sub>4</sub> flux that was recently derived from landscape scale measurements at Stordalen mire in northern Sweden (68°20'N,

19°03'E). In this case, the relationship is based on continuous high-frequency year-round measurements made in 2006 and 2007 (Jackowicz-Korczyński *et al.*, *submitted*). Two different functions were derived based on fluxes originating from different parts of the mire, which are both described as today being primarily permafrost free.

The first function is based on substantially lower CH<sub>4</sub> fluxes originating from a section dominated by stands of tall graminoid vegetation. Approximately twice as high fluxes were measured from a section with a somewhat mixed vegetation composition and influenced by the shallow Lake Villasjön (0.17 km<sup>2</sup>, max depth 1.3 m). Function (2) was derived from these higher fluxes (Jackowicz-Korczyński *et al.*, *submitted*). Both functions are presented below:

$$\text{Low fluxes} \quad \text{CH}_4 \text{ (Ts)} = 1.43 e^{0.119 \text{ Ts}} \quad (1)$$

$$\text{High fluxes} \quad \text{CH}_4 \text{ (Ts)} = 1.68 e^{0.162 \text{ Ts}} \quad (2)$$

CH<sub>4</sub> = methane flux [mg m<sup>-2</sup> h<sup>-1</sup>]

Ts = Soil temperature at 3 cm depth [°C]

R<sup>2</sup> = 0.50 and 0.77 for the first and second function respectively.

The strongest statistical relationship was found between soil temperature and CH<sub>4</sub> fluxes during the summer season (2006: 2 June-1 September; 2007: 4 June-11 September). As in the case of the cross-site study by Christensen *et al.* (2003), at Stordalen mire, the water table was continuously high (water saturated soils) and no significant correlation was found between water table position and CH<sub>4</sub> flux.

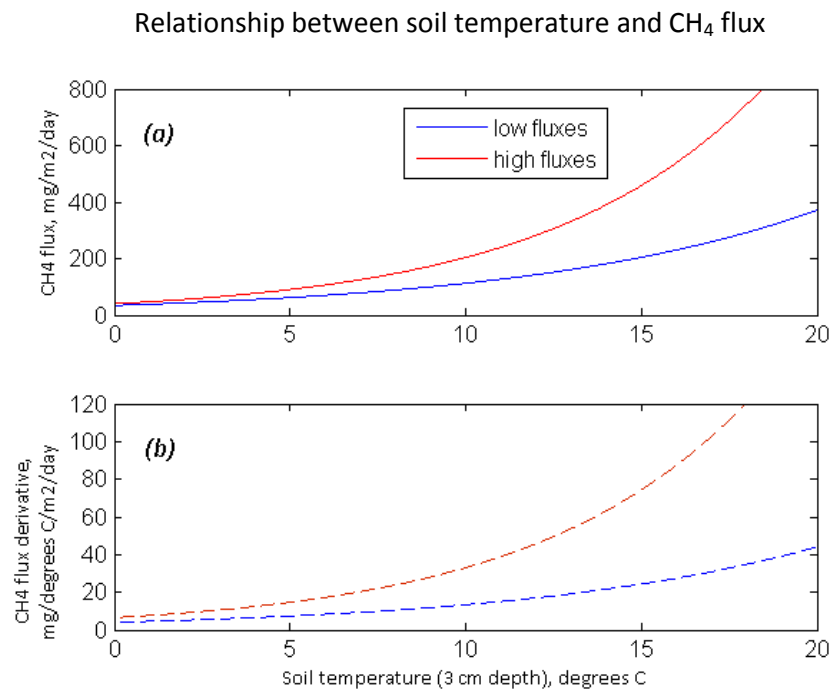


**Figure 2.3** The two temperature-flux relationships from Jackowicz-Korczyński *et al.* (*submitted*) are drawn in subplot (a) where the variables are converted into daily values. The red line is the higher emission function (2), and the blue line is function (1). Subplot (b) shows their derivatives with the same colour distinction.

The derivatives of functions (1) and (2) give the amount of CH<sub>4</sub> flux caused by a *change* in Ts (at a given soil temperature (Ts)). These functions are also drawn in Figure 2.3: subplot (b), and below they are converted into *daily* CH<sub>4</sub> flux (multiplied by 24 hours),

$$\text{Low fluxes} \quad [d\text{CH}_4(\text{Ts}) / d\text{Ts}] = 24 * 0.1702 e^{0.119 \text{ Ts}} \quad (3)$$

$$\text{High fluxes} \quad [d\text{CH}_4(\text{Ts}) / d\text{Ts}] = 24 * 0.2722 e^{0.162 \text{ Ts}} \quad (4)$$

$$[d\text{CH}_4(\text{Ts}) / d\text{Ts}] = \text{CH}_4 \text{ flux derivative } [\text{mg}(\text{CH}_4)^\circ\text{C}^{-1}\text{m}^{-2}\text{d}^{-1}]$$

Due to the exponential nature of the relationships, the derivatives increase with increasing soil temperatures, i.e. the sensitivity to Ts is higher when the soil is warmer. This implies that during the emission season, (anomalous) high temperatures have a larger impact on CH<sub>4</sub> emissions in summer when the soil is in general the warmest. In the measured flux data, it can also be seen that short-term variability in fluxes is the highest in summer time compared to spring, autumn, and winter (Jackowicz-Korczyński *et al.*, *submitted*).



## 3. METHOD

---

### 3.1 Overview

In the present study we make a new estimation of large-scale CH<sub>4</sub> emission anomalies from northern wetlands in order to compare them with atmospheric CH<sub>4</sub> growth rate data for the latitudinal region 53.1°N – 90°N. Primary focus lies on the 2007 growth rate event, however it will be evaluated in the context of overall interannual variation between 1992 and 2008. The emissions will be computed as a function of soil temperature anomaly by extrapolating two empirical soil temperature-flux relationships derived from measurements at Stordalen mire in northern Sweden. In theory, if the estimated total emission anomaly from wetlands corresponds to the CH<sub>4</sub> increase measured in the atmosphere, it would indicate that wetland emissions, to a large part, explains atmospheric CH<sub>4</sub> growth rate.

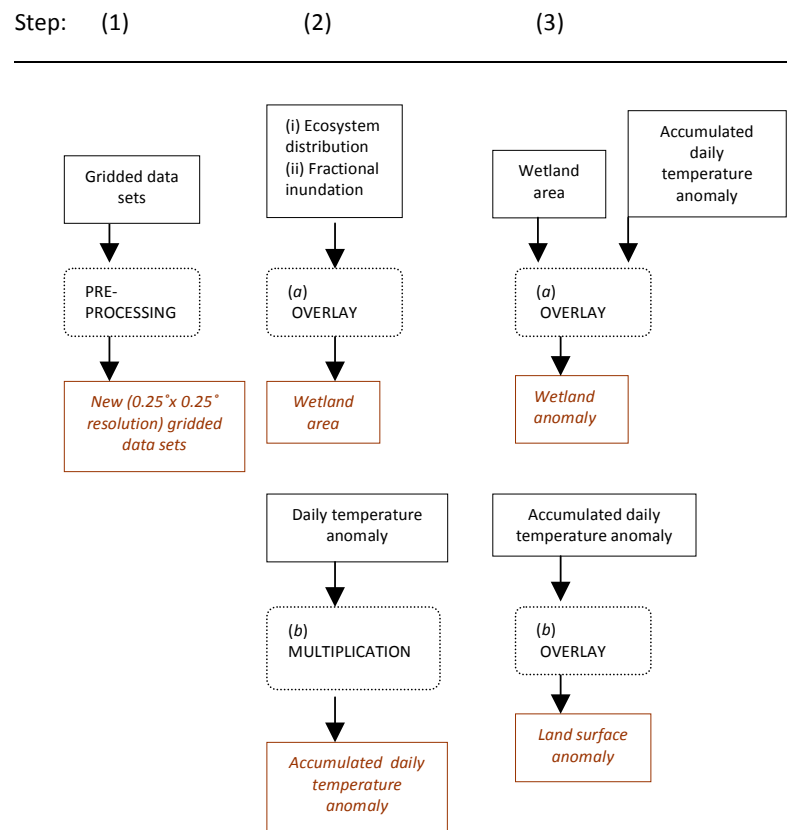
For the emission estimations, two main data types will be used: (1) *spatio-temporal temperature data*, and (2) *wetland distribution data*. Hence, temperature is the only driving environmental factor, which implies that the method is a generalized and oversimplified representation of the true dynamics of CH<sub>4</sub> flux from wetlands. Nevertheless, considering that repeated studies show a clear causal relationship between soil temperature and CH<sub>4</sub> emissions, particularly in high-emitting wetland ecosystems, temperature appears the most meaningful climatic variable to use in a first basic approach. This is done with the assumption that at all wetland sites used for the emission estimation, water table levels are at or near the surface. Positive results from this study would indicate that a more detailed study of this kind, including the influence of other factors, is of interest.

Within a given year, the analysis is limited to the annual period 16 May – 15 October, which is more or less representative of the growing season, at least in the more southern latitudes. This period will be referred to as the (*emission*) *analysis season*. The emission potential of wetlands naturally varies throughout the growing season due to the normal climatic seasonal pattern. Furthermore, since the applied sensitivity to soil temperature is exponential, in the emission estimation method, the impact of temperature anomalies on emissions (*anomaly impact* – see Section 3.4 for exact definition) is assumed to change as the season progresses. Trying to account for this feature (in a general sense), the computations will be performed on ½ month basis, i.e. there is a temporal resolution of 10 time periods over which the impact of temperature can vary. The exact periods are presented in Table I in the Appendix.

To make the progression of data processing and the computations easier to follow and understand, the method as a whole is summarized and presented in a chart in Figure 3.1. Part I includes the processing of wetland distribution and temperature anomaly, and Part II is thereafter concerned with the computation of CH<sub>4</sub> emission anomalies and the comparison of interannual variability between the atmospheric data and emission series. The different steps are described in more detail within the text.

Finally, a basic evaluation of the emission estimation method is also performed. This is however not included as a step in Figure 3.1.

Method Summary: **PART I**



**PART II**

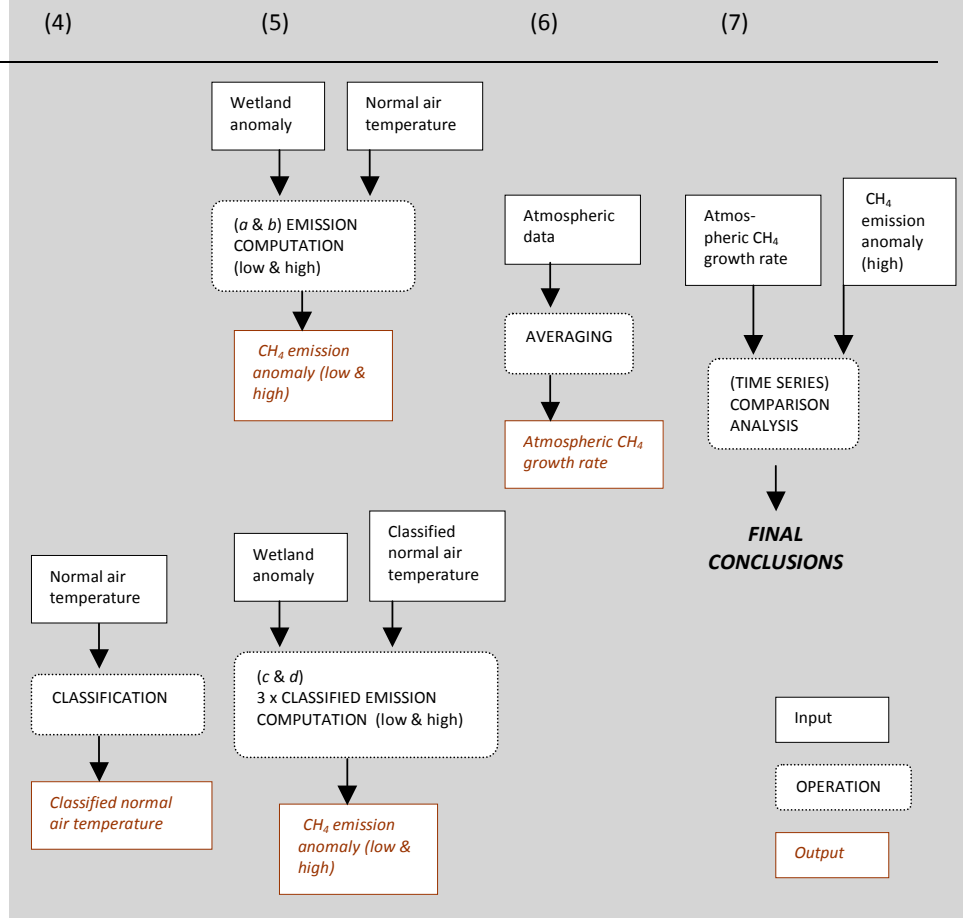


**Figure 3.1** The figure is a summary of the performed data processing and computations. A legend of the figure representations is displayed in the bottom right corner. The method as a whole is divided into Parts I & II, which together contain seven steps. Within each step there may be more than one operation (*a-c*). Note that the inputs used in one step are in most cases the outputs of operations in a preceding step. First, the spatial resolutions of the gridded data sets are made compatible, and the latitudinal zone of interest (53°N – 90°N) is extracted (step 1). Thereafter, in step 2, wetland area is derived from the two data sets in the *Matthews and Fung* wetland data base (2*a*), and temperature anomaly is moreover accumulated (2*b*). In step 3, the distribution of accumulated temperature anomaly is evaluated in relation to wetland area (3*a*), and land surface area (3*b*). In Part II, the actual CH<sub>4</sub> emission estimations are performed (step 5*a-d*). In the preceding step (4), normal air temperature is classified for application in the second emission computation approach (5*c & d*). In step 6, the atmospheric CH<sub>4</sub> growth rate data series is prepared for comparison with the computed CH<sub>4</sub> emission series (step 7). See Table 3.1 for more details about the original data.

### 3.2 Data

Gridded data of three variables are used in the analysis. They are: (1) daily air temperature anomaly, (2) normal daily air temperature, and (3) wetland distribution. These are in the format of latitude/longitude grids with global coverage. The anomaly data is the diverging temperature with reference to the second variable, i.e. the normal temperature for the period 1968-1996 (web source [4]). Information about source and resolution for all data sets is compiled in Table 3.1, and are thereafter further described in the bullet points that follow.

Wetland distribution (area) is obtained from a data base created by Matthews and Fung (1987). Five major wetland ecosystem groups are distinguished based on environmental characteristics associated with methane emission potential (Matthews and Fung, 1987). Two of these wetland groups are used in the present study; (1) *forested bog* and (2) *non-forested bog*.

**Table 3.1** A summary of information for the original data sets obtained for use in the analysis.

DATA	SPATIAL RESOLUTION	TIME RESOLUTION	TEMPORAL (annual) DATA COVERAGE	YEARS OF DATA	SOURCE
Daily air temperature anomaly	2.5° x 2.5°	10 of 15-16 day averages	16 May - 15 Oct.	1992-2008	NCEP/NCAR Reanalysis project, NOAA at PSD [4]
Normal daily air temperature, 1968-1996	2.5° x 2.5°	10 of 15-16 day averages	16 May - 15 Oct.		NCEP/NCAR Reanalysis project, NOAA at PSD [4]
Atmospheric CH <sub>4</sub> growth rate	Zonal mean for 53.1°N-90°N	48 time steps/year	Whole year	1992-2008	Compiled and provided by E.J. Dlugokencky, NOAA CMDL
Wetland data base:					Matthews and Fung, 1987
<i>Ecosystem distribution</i>	1° x 1°		Constant over time		(NASA GISS) [3]
<i>Fractional inundation</i>	1° x 1°				

- The *wetland data base* consists of two data sets, (i) *ecosystem distribution* – containing information on the distribution of the five major wetland groups (cells are labelled depending on the prevailing wetland type), and (ii) *fractional inundation* – providing the fraction of wetland area within a specific grid-cell. Additional details about the data base is available in a technical memorandum by Matthews (1989).
- The *atmospheric CH<sub>4</sub> growth rate data* does not have a spatial distribution; each value is instead a zonal average for the latitudinal band 53.1°N – 90°N (E.J. Dlugokencky, personal communication, 23 April 2009). This data has a temporal resolution of 48 time steps per year, and covers the years 1992-2008. The data is provided by E.J. Dlugokencky at NOAA Climate Monitoring and Diagnostics Laboratory (Boulder, USA). Description of the sampling and measurement methods can be found in Dlugokencky *et al.* (1994a), and details on how the data is processed to create a matrix of surface mole fractions as a function of time and latitude is described in Dlugokencky *et al.* (1994b).

- The *temperature data* has a temporal resolution of 10 time steps over the analysis season 16 May – 15 October, this means that the daily values are ½ month averages. The periods are presented in Table I in the Appendix. The length of the periods was chosen on the basis of practicality in terms of data handling. The last four periods (16 August – 15 October) are freely defined as autumn. Furthermore, the analysis level (or pressure level) of the temperature data is 1000mb, which should represent near surface (sea-level) temperatures (web source [4]). The source of this data is the NCEP/NCAR Reanalysis project at NOAA/ESRL Physical Science Division.

### 3.3 Wetland area and temperature anomalies

Evaluating the distribution of temperature anomalies in relation to wetland area is done in the first part of the analysis, Part I. It is the foundation for the emission estimations that follow in Part II. The performed steps involved are described below, and the equations can be found in the Appendix.

First, wetland area is easily obtained by multiplying the *fractional (wetland) inundation* with the total surface area within each grid-cell (step 2a in Figure 3.1). As mentioned earlier, only two out of five wetland ecosystems are considered, and their distribution is found in the *ecosystem distribution* data set. Secondly, the average temperature anomalies are multiplied with the length (number of days) of the seasonal period in question, giving *accumulated temperature anomaly* (step 2b). It is important to note that the applied CH<sub>4</sub> flux dependency (in Part II) is based on a relationship to soil temperature, but since (spatial) soil temperature data is not available on such a large-scale, a linear correlation between variation in air and soil temperature is assumed. The slope coefficient is set to 0.5, which implies that:

- *1 °C air temperature anomaly corresponds to 0.5 °C soil temperature anomalies.*

In order to combine the spatial anomaly data with wetland area distribution, all gridded data sets are adjusted to have the same resolution (0.25° x 0.25°) in the pre-processing step (1). In this operation, no interpolation is used; instead the original cell-values are preserved. Here, the latitudinal zone of interest (53°N – 90°N) is also extracted.

Finally, in the third step (3a & 3b), wetland area, total land surface area, and accumulated anomaly are used to derive two “new” variables. The first, *wetland anomaly*, is used as a measure of the magnitude of temperature anomaly occurring at wetland sites. It is the product of wetland area multiplied with accumulated anomaly. In this early stage, the absolute value of wetland anomaly is in itself not relevant. It is rather the *relative* difference between the 10 seasonal periods (i.e when during the analysis season anomalies occur) as well as the interannual variation that is of interest. The second variable, *land surface anomaly* is obtained for comparison. It is the magnitude of temperature anomaly occurring on all land surfaces. The calculation of these two variables is repeated for all years over the time period 1992-2008.

### 3.4 Estimating CH<sub>4</sub> emissions

An important aspect of the computed CH<sub>4</sub> emissions is that they represent estimated *anomalous* emissions with regards to an unknown “normal emission” for the period 1968-1996. In this way, the emission values can later be directly compared to atmospheric growth rate anomalies.

The amount of emission that a temperature anomaly produces is calculated from the two derivative functions (3) and (4), presented in Section 2.4.2. This is referred to as the *anomaly impact*, here defined as:

- *The amount of CH<sub>4</sub> emission produced by a one-degree change in soil (peat) temperature on one square meter of wetland during one day. The unit is mg CH<sub>4</sub> °C<sup>-1</sup>m<sup>-2</sup>d<sup>-1</sup>.*

The (anomaly) impact factor is found by replacing T<sub>s</sub> (soil temperature) in the two derivative functions with the data variable *normal daily air temperature*, T<sub>N</sub> (see data set in Table 3.1, second row). Note that for a given period:

- *T<sub>N</sub> is used as an approximation of the normal or “current” daily soil temperature from which the temperature change (anomaly) occurs. See Section 2.4.2 for more detail.*

In the emission computation, with function (3) a low emission estimate is returned, and with function (4) a high emission estimate is returned.

Two different approaches are employed for finding the anomaly impact for a given location and period. The second and somewhat more simplified approach is employed in order to easily test the effect of higher and lower predefined anomaly impact values in the late season. The first approach is used in the emission computations labelled *5a* and *5b* in Figure 3.1, and the second is used in *5c* and *5d*.

#### 3.4.1 Finding anomaly impact - first approach

In the first approach, unique anomaly impacts for each grid-cell and period are calculated as a function of the original T<sub>N</sub> data values. The behavior of the derivative functions is demonstrated in the following example. In computation *5b*, where the high emission function (4) is employed, if normal temperature [T<sub>N</sub>] = 15°C, the anomaly impact will be 74.2 [mg CH<sub>4</sub> °C<sup>-1</sup>m<sup>-2</sup>d<sup>-1</sup>]. If instead T<sub>N</sub> = 5°C, the anomaly impact will be 14.8, almost five times smaller. Since normal temperature varies over the season, so will the anomaly impact. On the other hand, it remains constant from one year to the next.

Finally, to obtain *CH<sub>4</sub> emission anomaly*, the anomaly impact is multiplied with the variable wetland anomaly (computed in step *3b* in Figure 3.1), which is the product of wetland area and accumulated temperature anomaly. However, when the normal temperature is below 5°C, no emission is computed (see Discussion for further explanation). The two functions are used in order to compare a conservative emission estimate with a more generous one. As with the variables in

Part I, emissions are computed for each year over the time period 1992-2008. See Appendix for equations.

### 3.4.2 Finding anomaly impact - second approach

In the second approach the normal temperature ( $T_N$ ) is first classified into five classes (step 4 in Figure 3.1). The classification scheme is presented in Table 3.2. Thereafter, in the emission computations that follow (5c & 5d), each class is associated with a predefined anomaly impact. These are simply the mean impact values for the temperature ranges used for the classification, calculated from the same derivative functions as in the first approach (see also Table 3.2 below).

**Table 3.2** In the second emission estimation approach, normal temperature is classified and associated with predefined anomaly impact levels. These impacts are averages for the same normal temperature ranges as the ones used in classification scheme. The *low* values are averages calculated with derivative function (3), and *high* values are calculated with derivative function (4) (see Section 2.4.2).

Class/Level	Normal temperature class ranges	Anomaly impact [mg CH <sub>4</sub> °C <sup>-1</sup> m <sup>-2</sup> d <sup>-1</sup> ]	
		<i>High</i>	<i>Low</i>
1	$T_N < 5^\circ\text{C}$	0	0
2	$5^\circ\text{C} \leq T_N < 10^\circ\text{C}$	24	11
3	$10^\circ\text{C} \leq T_N < 15^\circ\text{C}$	55	19
4	$15^\circ\text{C} \leq T_N < 20^\circ\text{C}$	123	35
5	$20^\circ\text{C} \leq T_N$	231*	56*

\*The highest impact factor is in fact the mean derivative for  $20^\circ\text{C} \leq T_N < 23^\circ\text{C}$

With this approach, three different “settings” are tested for computing CH<sub>4</sub> emissions. The variation is made in the anomaly impact scheme for the four last periods of the season (16 August – 15 October) – corresponding to a freely defined autumn. In the first “reference” setting the autumn anomaly impacts remain unchanged (i.e. as they are in Table 3.2); hence the impact scheme is uniform throughout the entire season. In the second setting the autumn impact is amplified, and in the third, the impact is reduced. The different settings can be viewed in Table II in the Appendix.

## 3.5 Comparing estimated emissions with atmospheric data

In order to relate estimated CH<sub>4</sub> emission anomalies with the atmospheric data, the seasonal (mean) atmospheric CH<sub>4</sub> growth rate corresponding to the analysis season (16 May – 15 October) is calculated (step 6 in Figure 3.1). This is done for all years in the period 1992-2008. The data values represent zonal average growth rates for the (circumpolar) latitudinal region 53.1°N-90°N. As a part of this operation, the growth rate value for 2007 is also converted into the amount of CH<sub>4</sub> increase in Tg CH<sub>4</sub>/year required to produce the observed growth rate in atmospheric concentration. The conversion factor used is 2.737 Tg/ppb (Fung *et al.*, 1991).

Finally, the last step of the method as a whole is to compare the computed CH<sub>4</sub> emissions with the atmospheric data (step 7). In the process of creating time series that are comparable with one another, the spatial data grids are summed across latitude and longitude, so that there is an accumulated total value for each year. In addition, any existing trends in the time series are removed. This means that the absolute values lose their significance and it is in fact the *relative* interannual variability that is the subject of analysis. Furthermore, the comparison is also extended to consider three latitudinal sub-series separately (see below).

#### Latitudinal sub-series

- 53°N - 60°N
- 60°N - 67.5°N
- 67.5°N - 90°N

The data series for the period 1992-2008 are compared looking for a potential relation in *relative interannual variation*. Indications of covariation with the atmospheric CH<sub>4</sub> growth rate are evaluated through plotting over time. The potential strength of a correlation is also evaluated by scatter plotting the annual atmospheric data values against the annual emission values.

### 3.6 Evaluating the CH<sub>4</sub> emission computation model

In order to evaluate the study results, it is necessary to have an idea of how the emission computation model performs. With focus on two spatio-temporal features of the estimation method, the following evaluation procedures are done.

- 1) First, a linear regression analysis is performed on the dependency of computed CH<sub>4</sub> emission anomalies on input temperature anomalies. One period at a time, the whole season total emission output of all years in the time series (17 values) are plotted against the corresponding total accumulated temperature anomalies (occurring on wetland areas). The slope of the regression is a type of “average” temperature sensitivity for the whole study area resulting from the applied computation model.
- 2) Secondly, since areas with a normal temperatures < 5°C are excluded from the computation of CH<sub>4</sub> emissions, for each period, the percentage of total wetland area available for emissions is calculated. This gives a comprehension of how the method feature in question may influence the results.



## 4. RESULTS

---

### 4.1 The strength and distribution of temperature anomalies

Because temperature is used as the driving environmental factor for wetland CH<sub>4</sub> emission, it is of interest to look at the development of large-scale warming occurring on wetland areas over time. This is represented by the variable *wetland anomaly*. For comparison, a measure of overall warming on *all land surfaces* is also presented in Figures 4.1a and 4.1b. In these figures, the spatial data values from the entire areal extent of the circumpolar north between 53°N – 90°N have been summed up into one value for each year.

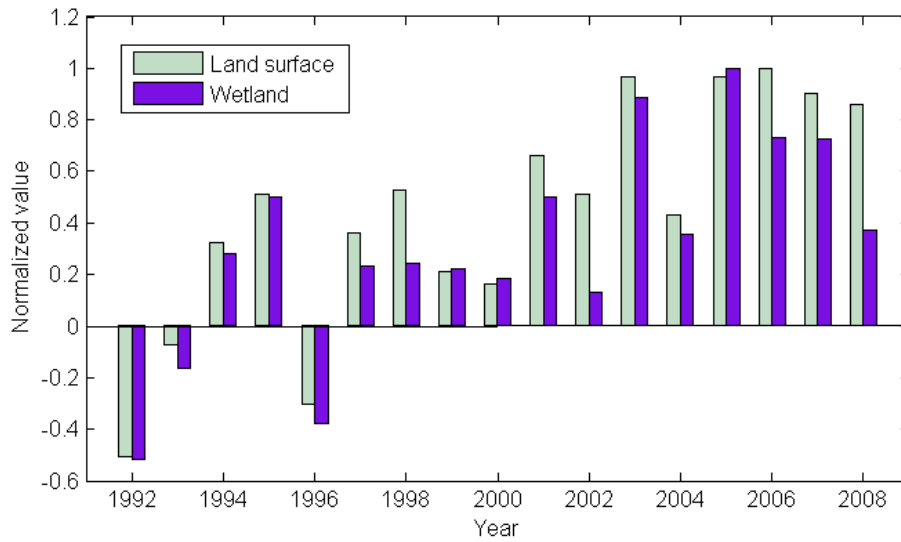
For the time period 1992-2008, considering temperature anomalies accumulated for the whole analysis season (16 May – 15 October), there is a clear increasing trend over time (Figure 4.1a). However, a more significant and lasting warming seems to begin first in 2003. In general, there is not much difference between the interannual variation of the *land surface* and the *wetland* series, with the exception of three years – 1998, 2002, and 2008. In these years, the (relative) warming over land is significantly larger than the warming occurring over wetland areas. The land surface series displays a minor peak in 1998, while the wetland series does not. The most interesting feature of the whole season time series is the absence of an outstanding warming event in 2007, at least in relation to preceding years. Such a warming was expected with regard to the initial idea that the 2007 growth rate peak was caused by high anomalous wetland CH<sub>4</sub> emissions, which in turn were the result of unusual high temperatures.

Since the method used to compute CH<sub>4</sub> emission is sensitive to *when* temperature anomalies occur, the intra-seasonal temporal distribution of anomalies was analysed more in depth. It was found that the only seasonal periods during which 2007 warming exceeds other years (peaks) is in July, see Figure 4.2 for visualization. Because July is in general the warmest month of the summer, anomalously high temperatures during this time can be expected to have high impact on wetland CH<sub>4</sub> emissions. Therefore July results are considered separately alongside the results from the analysis season as a whole.

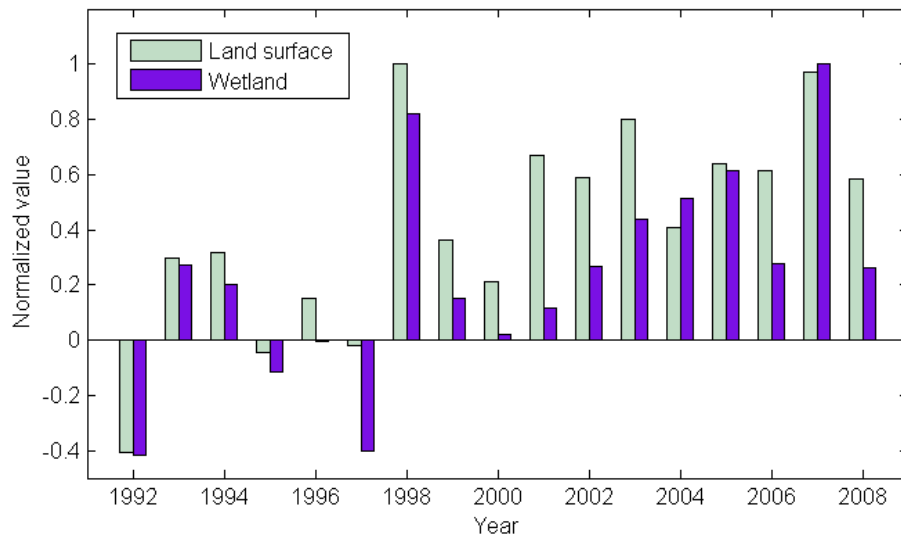
Figure 4.1b displays the July time series for both wetland and land surface anomalies. The 2007 peak is more pronounced in the case of wetland anomalies, as the values for year 2006 and 2008 are lower than those of the land series's. Other discrepancies between the two series occur in 1997, and over the five-year period 1999 – 2003.

## Normalized accumulated temperature anomalies

Whole analysis season (a)



July (b)



**Figures 4.1a and b** The diagrams show the development of accumulated temperature anomalies occurring over wetland areas as well as over all land surfaces over the time period 1992-2008. (a) is the seasonally (16 May – 15 October) accumulated values, and (b) is the July accumulated values. The values are normalized (division by the highest value in time series), but the original units are  $^{\circ}\text{C m}^2$  wetland area and  $^{\circ}\text{C m}^2$  land area respectively.

In the process of analysing the distribution of temperature anomalies within each season (intra-seasonal), a few interesting features were found. Apart from the 2007 July peak in wetland anomalies, in the four years preceding 2007, remarkably strong warming occurs during the later part of the season, see Figure 4.2. To a lesser extent, unprecedented early season warming also occurs within the range of these years. The implication of this early and late season warming could perhaps be a lengthening of the season. One can speculate if the warming pattern in directly preceding years could contribute to elevated CH<sub>4</sub> emissions anomalies in 2007.

Intra-seasonal temporal distribution of accumulated (normalized) wetland anomalies

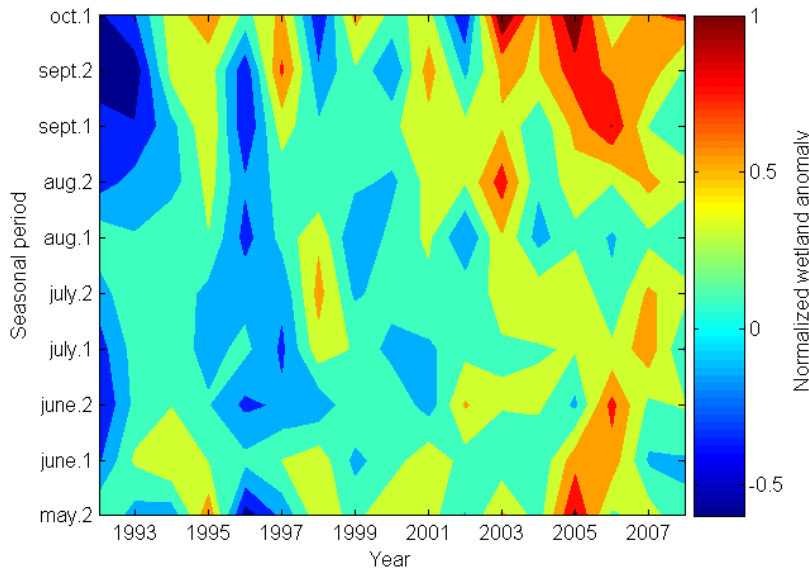


**Figure 4.2** The diagram shows a three-dimensional contour plot of the ten step temporal distribution of wetland anomaly within the emission analysis season and its development over time, from 1992-2008. It is created from 10 x 17 discrete normalized data values.

#### 4.2 Estimated CH<sub>4</sub> emission anomalies and atmospheric growth rate for 2007

Year 2007 is the only year for which the absolute values of estimated CH<sub>4</sub> emissions are considered for direct comparison with the measured atmospheric CH<sub>4</sub> growth rate. The emission estimations were computed with two slightly different approaches, and with each approach, a *high* and *low* estimate was produced. Moreover, in the second approach, where a classification scheme was used for assigning anomaly impact on emission (see Method for details), a variation in autumn anomaly impact gives four extra seasonal estimations (set.2 & set.3). All the different estimations are presented in Table 4.1. The values are summed totals for the entire areal extent of the circumpolar north between 53°N – 90°N. As with the variable *wetland anomaly*, in addition to seasonal totals, results for July are also considered and displayed in the same table. These July emission estimations alone stand for more than half of the seasonal totals. It is hard to say if this is a reasonable contribution level, but the indication that July may be very important supports further consideration of the relative interannual variation of July emissions alone. These results are presented in the next section.

The purpose of the 2007 CH<sub>4</sub> emission estimates from wetlands is to compare how they relate to the CH<sub>4</sub> emission amount required to produce the observed atmospheric growth rate. From the original atmospheric data, the mean CH<sub>4</sub> growth rate for the emission analysis season in 2007 was found to be 14.8 ppb/year. This is the zonal mean for 53.1°N – 90°N. This value converts into an input of approximately 41 Tg/year of extra CH<sub>4</sub> into the atmosphere (according to conversion factor by Fung *et al.*, 1991).

**Table 4.1** The estimated CH<sub>4</sub> emission anomalies accumulated for the whole analysis season, referred to as “seasonal”, and thereafter for July alone. The *high* and *low* estimations differ in the original temperature-flux relationship employed in the computation. In the second approach, set.1-3 differ in the setting of the anomaly impact for the four last periods (16 August – 15 October) (see Method for details).

Computation type	2007 estimated emission anomalies [Tg CH <sub>4</sub> ]			
	First approach		Second approach	
	<i>High</i>	<i>Low</i>	<i>High</i>	<i>Low</i>
Seasonal (ref. / set.1)	8.99	3.00	10	3.22
Seasonal (set.2)	-	-	12.5	3.83
Seasonal (set.3)	-	-	8.63	2.74
July	5.78	1.77	6.38	1.88

Depending on the computation approach and settings, the high emission estimates reach 21-30% of the estimated amount required to produce the measured atmospheric CH<sub>4</sub> growth rate (41 Tg (CH<sub>4</sub>)). The *low* seasonal emission estimations only amount to 7-10% of the required CH<sub>4</sub> emissions. It is clear that with the simple estimation method applied in this study, CH<sub>4</sub> emission anomalies estimated for 2007 do *not* reach the required magnitude to explain the 2007 atmospheric growth rate peak. There are of course many sources of uncertainties, which will be further addressed in the Discussion.

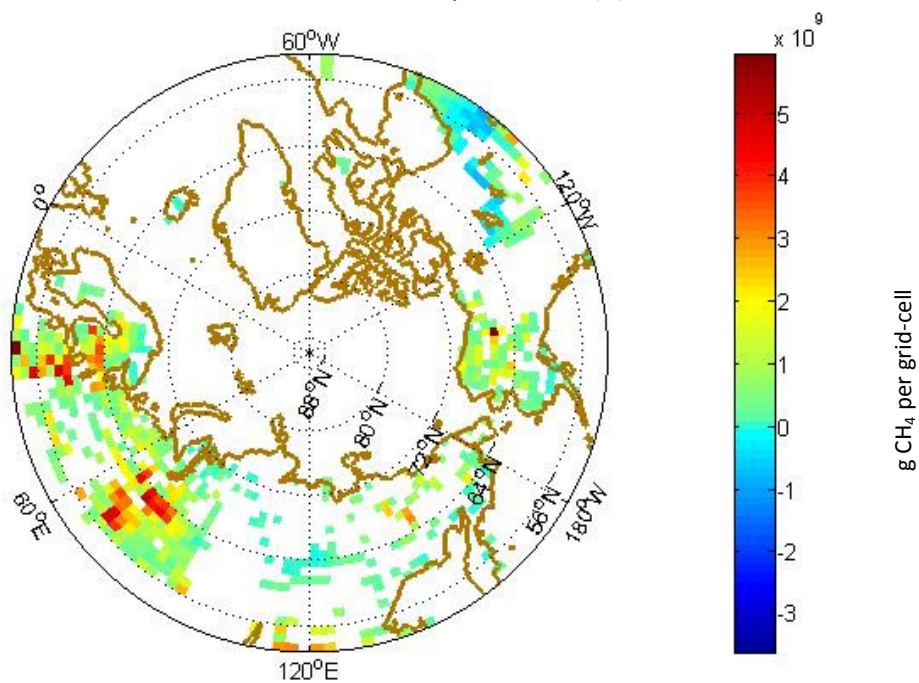
Beyond the summed total emission values presented above, it is interesting to see from *where* these emissions originate. Therefore the spatial distribution of the computed CH<sub>4</sub> emissions between 53°N – 90°N is presented in figures 4.3a and b with the unit *grams of CH<sub>4</sub> emission anomalies per grid-cell*. It is necessary to point out that the observed spatial pattern is dependent of the accuracy of the applied static wetland data base. But it is also the result of the spatial distribution and timing of temperature anomalies as well as the computation model.

In case of CH<sub>4</sub> emissions accumulated for the whole analysis season, there appears to be three major regions contributing with large emissions (see Figure 4.3a). Starting from the west, there is the *Northern European lowlands* (ca 20°E – 45°E), including northern Sweden, Finland, northeastern Europe and western Russia. Secondly, there is the *West Siberian Lowlands* between 60°E – 90°E, and finally, to a smaller extent, Alaska in North America also displays considerable extra CH<sub>4</sub> emissions.

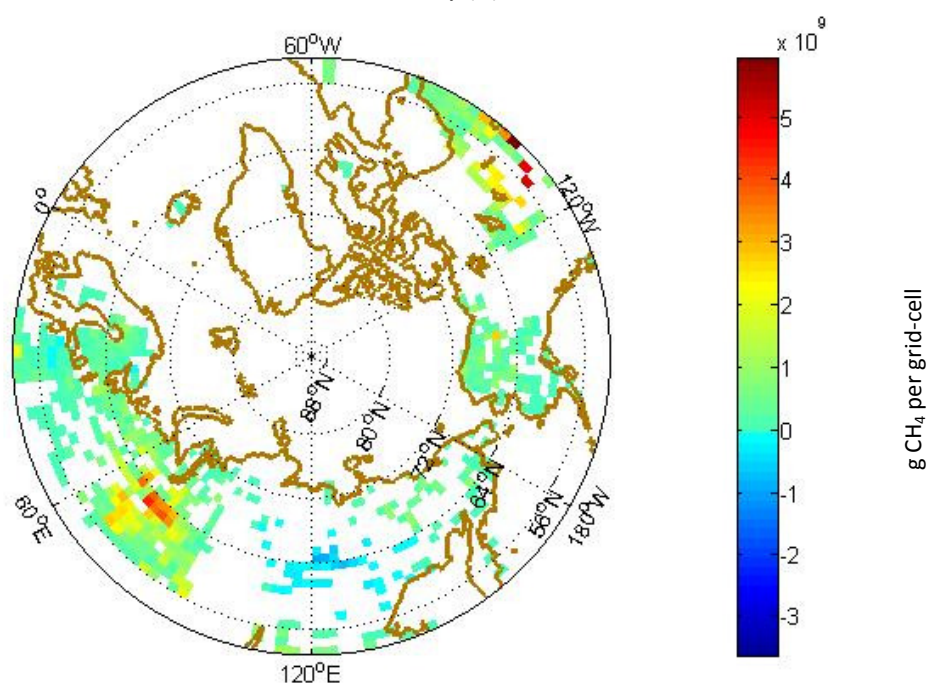
The spatial distribution of estimated CH<sub>4</sub> emission anomalies for July looks different (see Figure 4.3b); here the Siberian lowlands stand out as the dominating source of emissions, while the European lowlands display low emissions. Furthermore, a new emission hot-spot region becomes visible – *Central Canada*.

Spatial distribution of estimated CH<sub>4</sub> emission anomalies for 2007

Accumulated for the whole analysis season (a)



Accumulated for July (b)



**Figures 4.3a and b.** The spatial distribution of whole season and July accumulated CH<sub>4</sub> emission anomalies between 53°N – 90°N. The images are produced with the output of the *high* estimation with the first approach.

### 4.3 Comparing relative interannual variation, 1992-2008

By considering the 2007 CH<sub>4</sub> emission estimations in the context of a time series from 1992 to 2008, they are evaluated *in relation to other years*. All years in the series can be considered prone to the same unknown uncertainties. If indications of covariation in interannual variability are found between the atmospheric CH<sub>4</sub> growth rates and that of the estimated wetland emissions, it would strengthen the likelihood that the hypothesized dependency does exist for the 2007 peak event. The results of the comparisons are presented below.

Because there is a general increasing trend in temperature anomalies, originally, the computed emission series also showed an increasing trend over time. In contrary, the global atmospheric CH<sub>4</sub> growth rate displays an overall *decreasing* trend (Dlugokencky *et al.*, 2003). However, in the case of the northern latitudinal zone considered, this trend – if existing – appears very weak, at least in the data used in this study. In order to perform a better comparison analysis with focus on interannual variability, all the presented results are of detrended data series. This means that the absolute values are not relevant. Instead, it is the *relative* interannual variability that is being compared. Although there is a substantial difference in emission magnitude between the *high* and *low* emission estimations (see Table 4.1), not much difference is found in terms of interannual variability for the period 1992-2008. Therefore, only series of the high estimates are presented.

The time series of whole season accumulated CH<sub>4</sub> emissions computed with the second approach are presented in Figure 4.4 together with the atmospheric CH<sub>4</sub> growth rate. Observe that the growth rate is plotted on a secondary axis. The three emission series represent different scenarios of late season (autumn) anomaly impact on methane emission. *Setting 1* is a reference computation where the anomaly impact scheme is uniform throughout the whole season (as in the first approach). In *setting 2*, the impact of temperature anomalies have been elevated for autumn, and in *setting 3*, they have been reduced.

The main motivation for performing this simple testing of different autumn emission scenarios is that an early evaluation of the computation model showed that the actual sensitivity to temperature anomalies (anomaly impact) in the late season is very low (see discussion in Section 4.4). Consequently, for high temperature anomalies in autumn the method produces emission outputs that may be underestimations. Secondly, the original temperature-flux relationships applied for the computations tend to underestimate late season fluxes (Jackowicz-Korczyński *et al.*, *submitted*). In addition, field measurements of CH<sub>4</sub> fluxes from northern wetlands have shown that for the same soil temperatures, fluxes are higher in late season compared to early season (Christensen, 1993). It is not certain exactly what causes and controls these autumn elevated fluxes, but the observation gives reason to suspect that autumn fluxes may be an important component that contributes largely to the interannual variation of total emissions.

No matter the autumn impact setting, an important feature present in all three seasonal emission series in Figure 4.4 is that a relative peak in 2007 is absent. Apart from this, the growth rate dip in 2004 is fairly well represented in terms of an emission decrease, as well as the 1998 peak. In 2008, estimated emissions decrease drastically as does the atmospheric CH<sub>4</sub> growth

rate. The reference setting series is almost identical to that of the first computation approach, which is therefore not included in the figure.

Looking at how the three emission series in Figure 4.4 differ, it appears that increasing autumn impact (setting 2), somewhat *increases* the discrepancy between relative interannual variation of the estimated emissions and the atmospheric growth rate. For example, this is particularly apparent in 1995 and 2003. In contrary, when the autumn impact is the lowest (setting 3), the discrepancies appear to decrease. It is certain that the controls of the late season fluxes are more complex than represented here. It could be that late season fluxes are not so sensitive to *direct* soil temperature, as is assumed in the computations. Christensen (1993) suggested that the magnitude of late season fluxes may instead be a function of *progressing season* (see Discussion). In that case, one could speculate that if strong warming occurs during peak season (July & August), it may increase late season fluxes, more or less independent of immediate soil temperature conditions. This idea redirects interest to the appearance of the relative interannual variation of the estimated *July* CH<sub>4</sub> emissions, which will be discussed next and can be viewed in Figure 4.5.

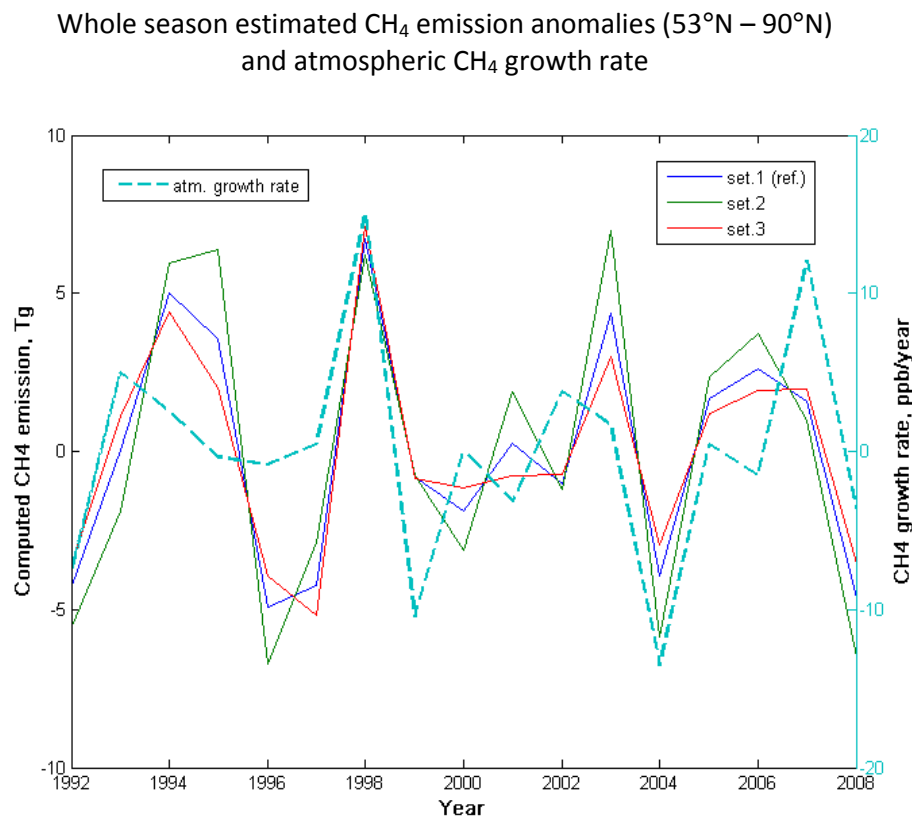


**Figure 4.4** The atmospheric CH<sub>4</sub> growth rate (53.1°N – 90°N) is compared to three series of computed CH<sub>4</sub> emissions accumulated for the whole season (second approach/high estimates). All series are detrended, which means that the values displayed on the axes are not the ones originally computed. The three solid lines differ in anomaly impact for the last four periods (autumn).

July estimated CH<sub>4</sub> emission anomalies (53°N – 90°N)  
and atmospheric CH<sub>4</sub> growth rate

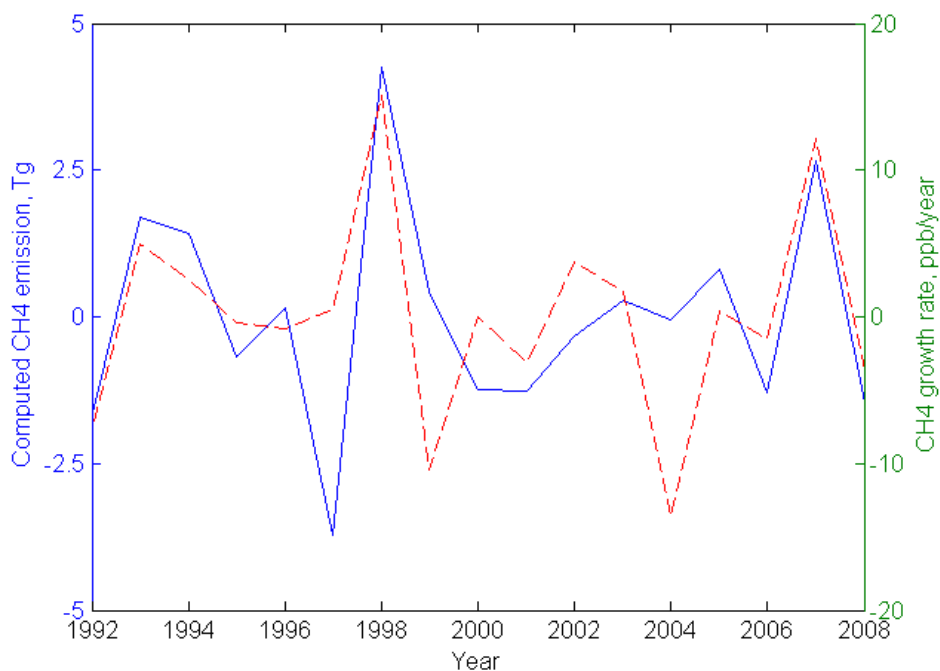
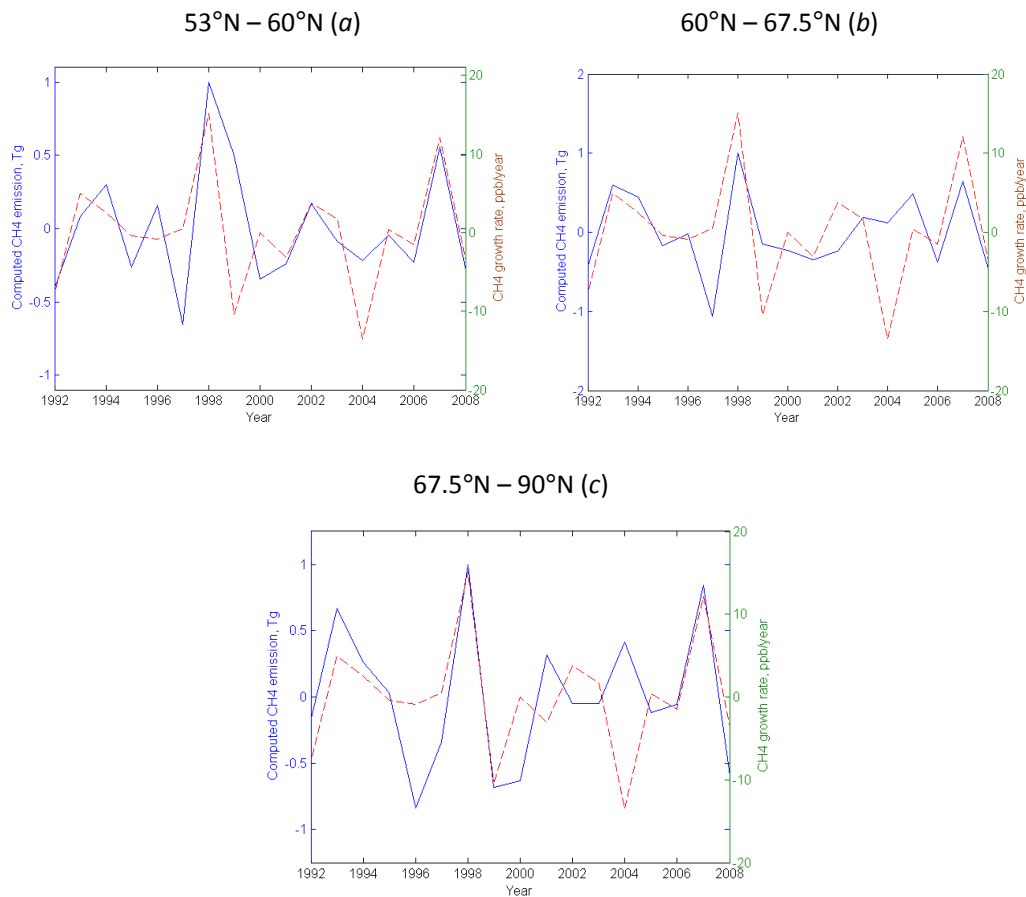


**Figure 4.5** The relative interannual variability of atmospheric CH<sub>4</sub> growth rate (dashed line) is compared to computed CH<sub>4</sub> emissions accumulated for July alone (first approach/high estimates) (solid line). Both series are detrended, which means that the values displayed on the axes are not the ones originally computed.

Whereas the series of whole season estimated emissions fail to peak in 2007, the July emissions display a remarkable fit with the (relative) interannual variability of the atmospheric growth rate data from 2006 to 2008, creating a nice peak in 2007 (see Figure 4.5). In general, it seems that for the more pronounced growth rate peak events (1993-94, 1998, and 2007) the computed emission anomalies (caused by high temperature anomalies) also peak. However, problems arise when lower temperature anomalies and low growth rate events occur. It is in these cases that the largest discrepancies between the emissions and atmosphere present themselves (e.g 1997, 1999, and 2004). An exception to this observation is the smaller peak in 2002-03, which is missing in the July series (although, present in the seasonal series). However, when the July series is split into smaller latitudinal sub-series, see Figures 4.6a-c, the peak in question does appear in the most southern latitudinal series in Figure 4.6a. In addition, for different smaller sections of the whole time series, the fit with the atmospheric data seems to improve in the sub-series. Disregarding year 1996, this is the case for the most northern latitudinal series (c), from 1992 to 1999. And, disregarding year 2004, the same can be said for series (a), from 2001 to 2008.

## Latitudinal sub-series of July estimated CH<sub>4</sub> emission anomalies



**Figures 4.6a-c** The estimated CH<sub>4</sub> emissions anomalies for July are presented in three latitudinal sub-series. The emission series are displayed as solid blue lines and the atmospheric series is the red dashed line.

From the results of the comparison, one can say that there does seem to exist some kind of dependency between the relative interannual variation of estimated wetland CH<sub>4</sub> emissions and the atmospheric data series. This indication becomes stronger when July emissions are considered separately. Of course, CH<sub>4</sub> emission from July can by itself only be expected to contribute with a portion, however a large portion, of the total seasonal or annual wetland emissions. In other words, emissions from July could not for any year make up the required emission amount needed to produce the observed atmospheric growth rate. However, the positive results for July still suggest that the temperature conditions during peak season may be pivotal – both because of its direct contribution with high emissions and perhaps indirectly by having an impact on the magnitude of emissions from the later part of the season.

When the growth rate data series are plotted against the emission series in Figures 4.7a and b, the indication of a correlation becomes more apparent. In (a) the points are quite well spread, but there appears to be a small, however still clear, correlation with large residuals. In (b), which contains the July emissions, three data points in the bottom left corner of the diagram deviate

largely from what could be interpreted as a linear regression. These points are the “low” years 1997, 1999, and 2004, already mentioned in connection with Figure 4.5.

### Computed CH<sub>4</sub> emissions anomalies vs. atmospheric growth rate

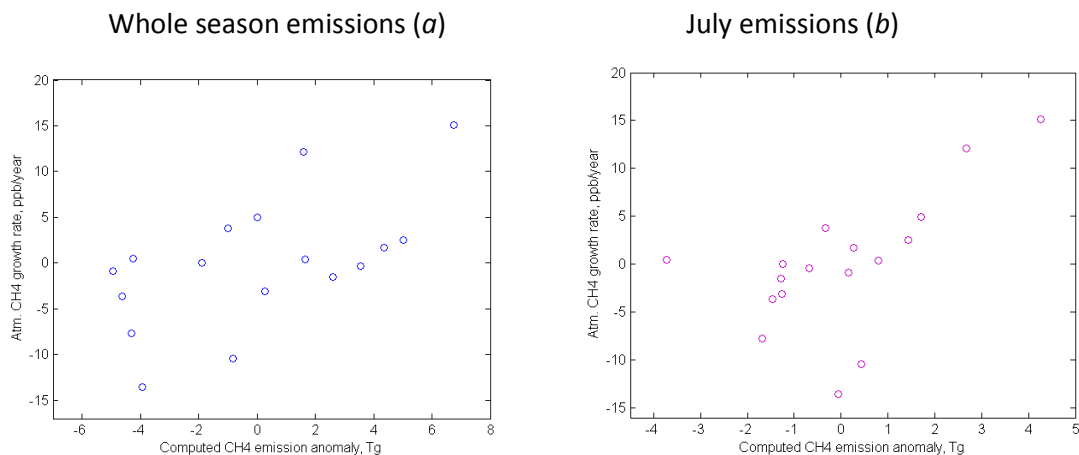


**Figure 4.7a and b** The emission estimations are plotted on the *x*-axis and the atmospheric growth rate is plotted on the *y*-axis. The used data values in (a) and (b) are from the detrended series in Figures 4.4 and 4.5 respectively.

It is obvious that the dependency between large-scale CH<sub>4</sub> wetland emissions and atmospheric CH<sub>4</sub> growth rate suggested by the presented results is in reality a very complex phenomenon. The largest discrepancies show that there must be other dependency factors involved that also control the interannual variation of atmospheric CH<sub>4</sub> growth rate in the circumpolar north. It could be that the relevance of large-scale wetland emissions is manifested in some years but not in others, dependent of other environmental factors. More about this is mentioned in the Discussion.

## 4.4 Evaluation of the CH<sub>4</sub> emission computation model

A priority when developing the CH<sub>4</sub> emission computation model was to make emissions dependent on both *where* and *when* temperature anomalies occur, which was implemented by calculating the anomaly impact factor from normal soil temperature.

The results of the evaluation show that the temporal feature was to some extent successfully implemented. Presented in Figure 4.8 is an average anomaly impact value for each period; they are derived from linear regression analysis of total wetland anomalies for the whole season (*x*-value) and computed emission anomaly (*y*-value) from all years in the time series (using values of the second approach/reference setting). Considering each period separately gives the development of a type of average anomaly impact throughout the season. The impact (of anomaly) gradually increases from the first period, reaches a maximum in July, and then decreases till the final period. The highest impact, found in July, is 100 mg CH<sub>4</sub> °C<sup>-1</sup> m<sup>-2</sup> d<sup>-1</sup>. In the figure, one can also see that the impact values in the late season are substantially lower than the early season impact values. Consequently, the relatively high 2007 wetland anomalies that occur from the middle of

September to the middle of October give very low emission outputs. For better visualization of this consequence, wetland anomalies (magnitude of accumulated temperature anomaly occurring over wetland area) for 2007 are presented in the same diagram.

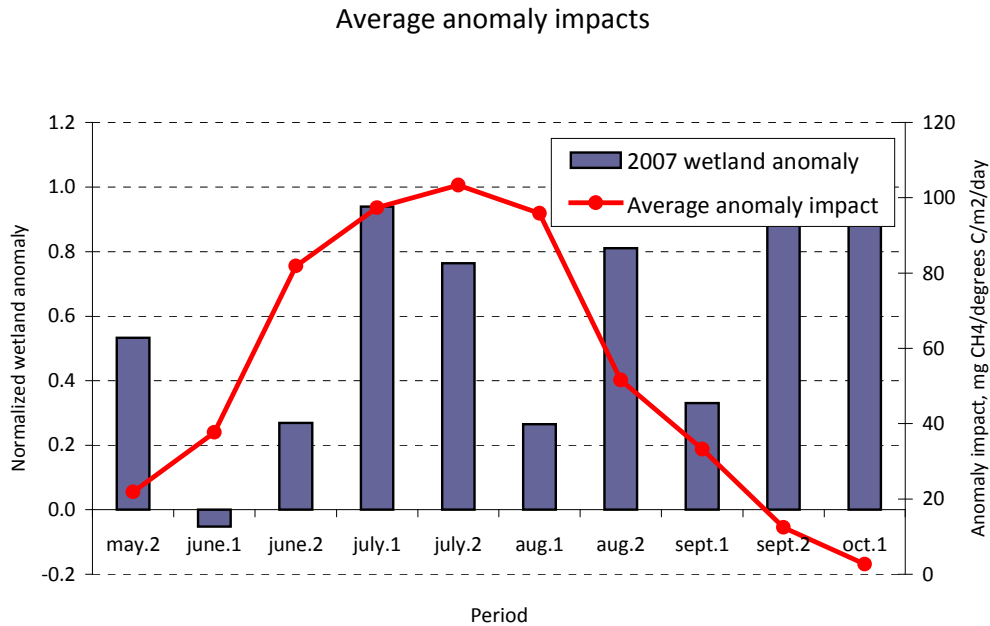


**Figure 4.8** The connected red circular markers in the diagram shows the average anomaly impacts that the emission computation model produces in the reference setting of the second approach (y-axis on the right side). To visualize how much weight the total temperature anomaly of each period is given as a consequence of these impact averages, 2007 wetland anomalies are also displayed as bars (y-axis on the left side).

These low autumn impacts are the result of low normal air temperatures (normal period 1968-1996), which in the computation model are used directly as an estimate for normal *soil* temperature. This temperature in turn decides the anomaly impact value in each grid-cell. Knowing that the late season may stand for a significant portion of total annual CH<sub>4</sub> emissions, one would expect that variations in these emissions to have a *proportional* influence on the overall fluctuations in large-scale wetland CH<sub>4</sub> emissions from one year to the next. With the used model, this is not the case. However, as described in the previous section, increasing the impact anomaly for the four last periods in a linear fashion does not seem to enhance the relative contribution of autumn emissions in the “right” way. This is concluded from the results of the comparison with atmospheric CH<sub>4</sub> growth rate (see Figure 4.4 and related discussion). The applied emission computation model is too simple to reflect a flux dependency that surely is much more complex.

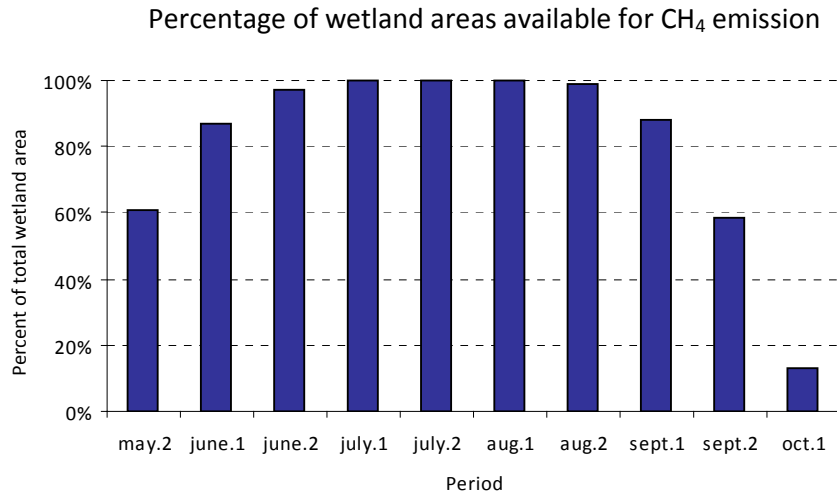


**Figure 4.9** The diagram shows the resulting percentages of total wetland area “switched on” for CH<sub>4</sub> emission in each period. The percentages are below 100% in the early and late season due the lowering of normal temperature. When normal temperature is below 5°C the model “switches off” the wetland.

Another feature of the model is the exclusion of emissions from grid-cells that have a normal temperature below 5°C. As a consequence, some wetland areas are “switched on” for emissions first in the first half of June, and are thereafter “switched off” in the second half of September and October. In Figure 4.9 it is clear that the late season is more strongly affected by this model restriction, which further diminishes the possibility for emission anomalies from the periods in question.

## 5. DISCUSSION

---

### 5.1 Evaluation of uncertainties in the method

The temperature-flux relationships used to derive the CH<sub>4</sub> emission estimations are based on measurements from a *single* site in northern Sweden. Extrapolating these over the entire circumpolar north is somewhat problematic. In reality, across the large study area, the character of the peat-rich wetland ecosystems will differ, and therefore also the conditions for CH<sub>4</sub> emission. However, a similar exponential relationship was found when measurements from multiple northern wetland sites were considered (Christensen *et al.*, 2003), which supports performing such a general extrapolation. For a more detailed study to be meaningful it would require more knowledge on regional or even local wetland environmental conditions and the dependency of CH<sub>4</sub> flux to soil temperature (as well as other factors).

Particularly interesting are the emission conditions in the *West Siberian lowlands*, because in our results for 2007, the distribution of estimated emissions suggest that this region is the single largest contributor to the total emission anomaly. Furthermore, when July is considered separately, the domination of the West Siberian lowlands is reinforced (see Figure 4.3a and b). Although these results are biased by the appearance of the used *Matthews and Fung* wetland data base (1987), the region is known to contain extensive areas of peatlands, and there are independent studies that have reported high CH<sub>4</sub> emissions from wetland ecosystems and lakes in the region (e.g. Takeuchi *et al.* 2003; Friberg *et al.*, 2003; Christensen *et al.*, 2003). This further indicates that anomalous warming over the West Siberian lowlands may be important also in terms of larger scale interannual variation in CH<sub>4</sub> emissions.

The extrapolation issue is furthermore related to the quality and availability of detailed and updated wetland data bases. The two wetland ecosystems that are extracted for the purpose of this study, *forested* and *non-forested bog*, are both described as peat-rich and high CH<sub>4</sub>-emitting ecosystems (Matthews and Fung, 1987). The data base is however fairly out of date, and with such a general ecosystem classification scheme it can be expected to contain inaccuracies. But for the purpose of this large-scale study, where the overall level of generalization is high, this data can be considered appropriate.

Evaluating the emission computation model in another aspect, there is an important discrepancy related to the simple assumptions made in order to use *air* temperature data for computing CH<sub>4</sub> emissions that are in fact sensitive to *soil* temperature (at 3 cm depth) (see Method for details). The conversion factor of 0.5°C soil anomalies for 1°C air temperature anomaly was applied after a fairly good empirical relationship was found between daily air and soil temperature data from Stordalen in northern Sweden (data provided by M. Jackowicz-Korczyński). As with the temperature-flux relationships, this simple representation may only be valid under limited soil conditions. Nevertheless, the fact that high air temperature anomalies will to some extent affect soil temperature, implies that despite this simplification, this emission estimation approach can still be considered to give valuable results, especially in terms of relative variations from one year to the next.

Because the found correlation (mentioned above) was limited to a period when daily air temperatures were continuously above 5°C, no emission outputs were computed when the *normal temperature* was below 5°C. According to the used temperature-flux relationship, the extra (anomalous) CH<sub>4</sub> emission caused by temperature anomalies would be very low at current or normal soil temperatures below 5°C (see Figure 1.2b). It therefore seemed reasonable to assume that within the boundaries of this study, impact of anomalies occurring at low temperatures do not have a major impact on the overall interannual variation. This is also why the length of the emission season considered was limited to 16 May – 15 October. However, another potentially important aspect that is not accounted for is a possible *lengthening* of the emission season due to the extreme temperature anomalies early or late in the season. If that is the case, it is a source of emission underestimation that may be inconsistent from one year to the next, affecting the interannual variability.

With a limited level of data accuracy available, there is an advantage with analysing a *time series* of emissions since the estimated values for each year, with primary focus on 2007, can then be considered in a relative sense. However, the time series is obtained by repeatedly applying the same computation model from year 1992 to 2008, which implies that the conditions for CH<sub>4</sub> emissions are automatically assumed constant from one year to the next. Only the distribution and magnitude of temperature anomalies vary. For example, over the time period 1992-2008, there may have occurred changes in wetland distribution. Due to climate warming, it is likely that shifts in wetland vegetation composition and hydrology in connection with permafrost melting in the sub-arctic region also causes changes in the CH<sub>4</sub>-flux dynamics (Johansson *et al.*, 2006). This was not accounted for as the emission time series were created. On the other hand, when 2007 is considered only in relation to the direct preceding and following years, changes in wetland distribution can be disregarded. In this case, other factors, such as *precipitation*, followed by variations in soil moisture (water table height), are probably more relevant.

Without going into detail, it should be said that the atmospheric CH<sub>4</sub> growth rate data is also the output of a model, followed by its own uncertainties. According to information given by the data provider Ed J. Dlugokencky (personal communication, 23 April 2009), the temporal resolution is not very reliable. As a consequence, the derived *season* mean values (16 May – 15 October) used for comparison with estimated wetland emissions, may not differ much from that of the *annual* mean values.

## 5.2 Comparing estimated CH<sub>4</sub> emission anomalies with atmospheric growth rate

One can say that the estimations of large-scale anomalous methane emissions for 2007 (3-12.5 Tg CH<sub>4</sub>, or 7-30% of required amount) are too low to attribute the zonal atmospheric CH<sub>4</sub> growth rate peak to CH<sub>4</sub> emissions from northern wetlands. However, considering the applied level of generalization in the estimation method, better results could not really be expected. It should be noted that the mismatch may also be the result of an *overestimation* of the CH<sub>4</sub> emission amount required to produce the observed growth rate, i.e. the applied conversion factor (from ppb/year to Tg CH<sub>4</sub>/year) is perhaps too high for use in the thinner high latitude atmosphere.

In the case of year 1998, our results are not far from comparable with the estimation of another study by Dlugokencky *et al.* (2001). From calculations with a global process-based model (using soil-temperature and precipitation anomalies as input data), the authors estimated an annual emission anomaly value of 11.6 Tg CH<sub>4</sub> for wetlands north of 30°N (compared to a calculated average for 1982-1993). In the current study the high estimate for 1998 is between 9-10 Tg CH<sub>4</sub> for the shorter period 16 May – 15 October, and the smaller latitudinal zone 53°N – 90°N.

Despite the initial low estimations for 2007, the results from the evaluation of *relative interannual variation* of emission anomalies from 1992 to 2008 are positive, strongly suggesting that there is a relation to atmospheric CH<sub>4</sub> growth rate. The correlation is improved when July is considered on its own. And, in the July series, wetland emissions peak in 2007, which in a relative sense correspond to the atmospheric growth rate peak. The 2007 peak is also consistently present in all July latitudinal subseries (see Figures 4.6a-c). However, there are somewhat too few data points to statistically confirm the correlations visible in Figure 4.7a and c.

Since temperature is the sole environmental variable that forces wetland CH<sub>4</sub> emission in this study, the variation in temperature anomaly from one year to the next is the foundation for the interannual fluctuations of estimated emissions. For the period 1992 – 2008, early results showed that there was an unprecedented warming over wetland areas in July 2007. This motivated the parallel analysis of CH<sub>4</sub> emission anomalies for the *whole season*, and then *July* separately. Considering that an equivalent warming peak was found for July 1998, it is interesting that the two most prominent atmospheric CH<sub>4</sub> growth rate peaks between 1992 – 2008 are almost exclusively reflected in July warming, both over wetlands and all land surfaces (see Figures 4.1a and b). (There is also a minor peak in terms of warming over all land surfaces for the whole season.)

With an awareness of the limitations and uncertainties of the CH<sub>4</sub> emission estimation method, considering July emissions on its own holds advantages. The original soil temperature-flux dependencies found at Stordalen were the strongest for the summer season (Jackowicz-Korczyński *et al.*, *submitted*), which therefore increases the credibility of estimating July emission variation as a function of soil temperature variation. Furthermore, real CH<sub>4</sub> emissions from wetlands are at their peak in July, and in the applied emission computation model, July is the period during which temperature anomalies has the highest impact on emissions (see Figure 4.8). This implies that although July only represents one fifth of the whole analysis season (16 May – 15 October), it has the potential of contributing with a large amount of the total anomalous emissions in a given year. Another advantage with considering July emissions is that there is less uncertainty with regards to changes in temperature sensitivity (anomaly impact) and environmental conditions that otherwise will occur as the season progresses. Due to the above mentioned positive aspects, we have more confidence in the interannual fluctuation of the July emission anomalies than that of the whole season. It is still problematic to explain or find a reason to why July emissions alone could be considered representative of the relative interannual variation of emissions on an annual basis. One possibility, which would be compatible with our results, is that there is a lagged dependency between peak season emission conditions and the magnitude of late season emissions. This goes in line with the suggestion that there in autumn is a “background” CH<sub>4</sub> flux that is dependent on the progression of season rather than immediate soil temperature (Christensen, 1993).

As pointed out in the Results section, there are important discrepancies in both the July and whole season emission series that should not be ignored. Consequently, it seems that the suggested dependency between emissions and growth rate is periodically interrupted. There are several possible explanations to why the estimation method may fail, considering its simplicity. Some years, soil temperature may not be the primary limiting environmental factor. As suggested by Christensen *et al.* (2003), in terms of large-scale variations the sensitivity to soil temperature is a feature that may be “switched off” when the water table falls below a threshold height. In other words, the water table height becomes the primary limiting factor of CH<sub>4</sub> flux, reducing emissions drastically. In order to account for such a behavior when estimating CH<sub>4</sub> emissions, it would be necessary to incorporate *precipitation* as an input variable in the method. It is furthermore likely that other sources also contribute to the growth rate in a given year, for example boreal fire. The relative source contribution may vary between years, depending on the conditions.

To some extent the noted discrepancies are visible as differences between anomalous warming over wetland areas and anomalous warming over all land surfaces (see Figure 4.1a and b). For example, in the July series that represents overall warming (*land surface anomaly*), there is a clear warming event 2001 to 2003, without an equivalent in the wetland series. The same event is also present in the case of *whole season* warming (Figure 4.1a). This indicates that another temperature sensitive methane source could have caused this minor CH<sub>4</sub> growth rate peak in place of wetlands. This source could be boreal fires, which has by previous authors been suggested the primary cause for the particular event in question (Simmonds *et al.*, 2005). Since one could expect fires to be sensitive to extreme warming on non-wetland land areas, our results appear to support such an explanation.

The wild fire source (and biomass burning) is furthermore highly relevant in terms of the 1998 growth rate peak. From our findings the question arises if high *July* temperatures in particular are relevant for the occurrence of fire, because otherwise 1998 does not appear exceptionally warm, at least not in the northern hemisphere between 53°N – 90°N. However, in the present study, data on extensive drought conditions that may have prevailed due to the strong El Niño event are not considered. Observing that the two years with the lowest CH<sub>4</sub> growth rates, 1999 and 2004, follow years where boreal fires have been suggested the dominating explanation for growth rate increase, perhaps extensive drought conditions during these events had an impact on the years that followed, limiting wetland emissions in a way that our model cannot account for.

Finally, to repeat an important aspect that makes 2007 unique in comparison to the 1998 and 2002-2003 growth rate peaks; no corresponding peak in atmospheric CO growth rate was measured in the northern high latitudes in 2007 (Rigby *et al.*, 2008; web source [2]). CO is also produced at the event of biomass burning and wild fires. If it increases in the atmosphere in conjunction with CH<sub>4</sub>, it supports the burning source theory. However, since such a peak was not found in 2007, the wetland source explanation is better grounded.

## 6. CONCLUSIONS

---

The findings presented in this study confirm a link between anomalous warming and atmospheric CH<sub>4</sub> growth rate in high northern latitudes. This can be concluded from the coinciding peak and dip events that are visible in time series for the period 1992-1998.

Assuming that the magnitude of large-scale variation in wetland CH<sub>4</sub> emissions are primarily (under saturated moisture conditions) controlled by soil temperature, the results also indicate that variations in annual wetland emissions could in fact explain, or contribute, to large parts of the annual atmospheric growth rate variations. We find that when the relative interannual variation of estimated July emissions (based on July temperature anomalies) are considered separately, the fit with the CH<sub>4</sub> growth rate series is in several ways improved. Most striking is the appearance of a pronounced emission peak in 2007, which is not visible as estimated emissions from the whole analysis season (16 May – 15 October) are considered.

On the one hand, this seems to strengthen the wetland source hypothesis, because in July, CH<sub>4</sub> emissions from wetlands are at their peak, and according to field measurements, the sensitivity to soil temperature appears to be highest during peak emission season. What other emission source could be sensitive, and so clearly linked, to *July* warming?

On the other hand, July alone cannot provide the amount of anomalous emissions necessary to produce the observed growth rates in a given year. One way to explain this contradiction is that the applied emission estimation method has some fundamental faults, and lack certain components that limits its capability to model, (1) how the relation to soil temperature in reality changes as the season progresses, and (2) how other environmental factors may limit emissions (e.g. precipitation and water table height). The second point becomes obvious due to the presence of years for which there are large discrepancies between the emission and atmospheric series (e.g. in 1997, 1999, and 2004), which could for example be linked to dryer soil conditions. In a basic model evaluation, the unclear contribution of late season emissions becomes particularly apparent.

In case of the 2007 growth rate event, in this study, the absolute CH<sub>4</sub> emission anomalies estimated from wetlands only reaches at the most 30% of the required amount necessary to explain the high atmospheric CH<sub>4</sub> increase. However, considering the discussed uncertainties regarding the estimation method, this does not immediately eliminate the possibility that anomalous high emissions from wetlands is the underlying reason for the high atmospheric growth rate over high northern latitudes in 2007. In contrary, the excellent relative peak in July estimated emissions point at the existence of a causal relationship that requires more exploration.

A definite outcome from this study is that the addressed research questions can and should be explored further. The applied approach works fairly well considering its simplicity, but it could be improved and developed in several ways, for example by incorporating precipitation or drought extension as factors that influence large-scale wetland CH<sub>4</sub> emissions. To move forward with regards to the *absolute value* of total annual (anomalous) emissions, it is necessary to find a somewhat more complex model in terms of how the controls of emissions changes over a growing season. Optimally, consecutive years of CH<sub>4</sub> flux measurements at high-emitting northern wetlands should be continued to improve the understanding of variations in environmental controls, and the

magnitude of variation in total annual CH<sub>4</sub> emissions, from one year to the next. With reference to our results, such measurements at wetland sites in the West Siberian Lowlands would be particularly valuable. Furthermore, using a new updated data base of the current extent of wetlands, for example based on satellite imagery, would also be of interest.

## *Acknowledgements*

It is a great feeling to finally finish this Master Degree thesis, and naturally there are several people to whom I need to give my thanks for in various ways providing me with support and making this end possible. First of all there is my supervisor in the project, Torben Christensen who first introduced me to the topic and “mystery” of interannual variation in atmospheric CH<sub>4</sub> growth rate, and has remained encouraging all the way through, always with an open mind for new ideas and solutions. I have also had practical help from other staff members at our department at Lund University; Marcin Jackowicz-Korczyński provided me with data and information from his research at Stordalen mire (northern Sweden) on which large parts of the thesis is based; and Margareta Hellström deserves thanks for always being approachable and helpful with issues concerning the monster software Matlab. I would also like to thank Ed Dlugokencky from NOAA Earth System Research Laboratory (Boulder, USA) and Elaine Matthews from NASA Goddard Institute for Space Studies for, through the middlehands of Torben, answering to our requests regarding the atmospheric and wetland distribution data.

Moving on to a more personal room, the people closest to me – family and friends, have given me everyday support, encouragement, and care. Among them, Lukasz Nowak also stood for technical expertise regarding some computer programming issues, which made it possible to move forward in the analysis. Thereafter, in the process of writing and re-writing the manuscript, I thank my father for taking time to read and comment on one version after the other, until I let it go.

## *Cited References*

- Blake D.R. and Rowland F.S.. 1988. Continuing worldwide increase in tropospheric methane, 1978 to 1987. *Science* **239**(4844). pp 1129-1131. Cited in IPCC 2007, Chapter 2.3.2.
- Bousquet P., Ciais P., Miller J.B., Dlugokencky E.J., Hauglustaine D.A., Prigent C., Van der Werf G.R., Peylin P., Brunke E.-G., Carouge C., Langenfelds R.L., Lathière J., Papa F., Ramonet M., Schmidt M., Steele L.P., Tyler S.C., and White J.. 2006. Contribution of anthropogenic and natural sources to atmospheric methane variability. *Nature* **443**. pp. 439-443.
- Chapin III F. S., Matson P. A., Mooney H. A.. 2002. *Principles of Terrestrial Ecosystem Ecology*. Springer Science+Business Media, Inc. NY, USA.
- Christensen T.R., Ekberg A., Ström L., Masterpanov M., Panikov N., Öquist M., Svensson B.H., Nykänen H., Martikainen P.J., and Oskarsson H.. 2003. Factors controlling large scale variations in methane emissions from wetlands. *Geophysical Research Letters* **30**(7).
- Christensen T.R., Prentice I.C., Kaplan J., Haxeltine A., and Sitch S.. 1996. Methane flux from northern wetlands and tundra – An ecosystem source modelling approach. *Tellus* **48B**. pp. 652-661.
- Christensen T.R.. 1993. Methane emission from Arctic tundra. *Biogeochemistry* **21**. pp. 117-139.
- Denman, K.L., G. Brasseur, A. Chidthaisong, P. Ciais, P.M. Cox, R.E. Dickinson, D. Hauglustaine, C. Heinze, E. Holland, D. Jacob, U. Lohmann, S Ramachandran, P.L. da Silva Dias, S.C. Wofsy and X. Zhang, 2007: Couplings Between Changes in the Climate System and Biogeochemistry. In: *Climate Change 2007: The Physical Science Basis. Contribution of Working Group I to the Fourth Assessment Report of the Intergovernmental Panel on Climate Change* [Solomon, S., D. Qin, M. Manning, Z. Chen, M. Marquis, K.B. Averyt, M.Tignorand H.L. Miller (eds.)]. Cambridge University Press, Cambridge, United Kingdom and New York, NY, USA.
- Dlugokencky E.J., Masarie K.A., Lang P.M., Tans P.P., Steele L.P., and Nisbet E.G.. 1994a. A dramatic decrease in the growth rate of atmospheric methane in the northern hemisphere during 1992. *Geophysical Research Letters* **21**. pp. 45-48.
- Dlugokencky E.J., Steele L.P., Lang P.M., and Masarie K.A.. 1994b. The growth rate and distribution of atmospheric methane. *Journal of Geophysical Research* **99**(D8). pp. 17,021-17,043.
- Dlugokencky E.J., Masarie K.A., Lang P.M., Tans P.P.. 1998. Continuing decline in the growth rate of the atmospheric methane burden. *Nature* **393**. pp. 447-450.
- Dlugokencky E.J., Walter B.P., Masarie K.A., Lang P.M., and Kasischke E.S.. 2001. Measurements of an anomalous global methane increase during 1998. *Geophysical Research Letters* **28**(3). pp. 499-502.
- Dlugokencky E.J., Houweling S., Bruhwiler L., Masarie K.A., Lang P.M., Miller J.B., and Tans P.P.. 2003. Atmospheric methane levels off: Temporary pause or a new steady-state? *Geophysical Research Letters* **30**(19).
- Forster, P., V. Ramaswamy, P. Artaxo, T. Berntsen, R. Betts, D.W. Fahey, J. Haywood, J. Lean, D.C. Lowe, G. Myhre, J. Nganga, R. Prinn, G. Raga, M. Schulz and R. Van Dorland, 2007: Changes in Atmospheric Constituents and in Radiative Forcing. In: *Climate Change 2007: The Physical Science Basis. Contribution of Working Group I to the Fourth Assessment Report of the Intergovernmental Panel on Climate Change* [Solomon, S., D. Qin, M. Manning, Z. Chen, M. Marquis, K.B. Averyt, M.Tignor and H.L. Miller (eds.)]. Cambridge University Press, Cambridge, United Kingdom and New York, NY, USA.
- Friborg, T., Soegaard H., Christensen T. R., Lloyd C. R., and Panikov N. S., 2003, Siberian wetlands: Where a sink is a source, *Geophysical Research Letters*, 30(21).

- Fung I., John J., Lerner J., Matthews E., Prather M., Steele L.P., and Fraser P.J.. 1991. Three-dimensional model synthesis of the global methane cycle. *Journal of Geophysical Research* **96** (D7). pp. 13,033-13,065.
- Hogan, K.B. and Harriss R.C.. 1994. Comment on 'A dramatic decrease in the growth rate of atmospheric methane in the northern hemisphere during 1992' by E. J. Dlugokencky et al.. *Geophysical Research Letters*, 21(22). pp. 2445–2446. Cited in Dlugokencky et al. (2001).
- Jackowicz-Korczyński M., Christensen T.R., Bäckstrand K., Crill P., Friborg T., Masetpanov M., and Ström L. *Submitted for publication*. Annual cycles of methane from subarctic peatland. *Journal of Geophysical Research* ???
- Johansson T., Malmer N., Crill P. M., Friborg T., Åkerman J. H., Masterpanov M., and Christensen T. R.. 2006. Decadal vegetation changes in a northern peatland, greenhouse gas fluxes and net radiative forcing. *Global Change Biology* **12**. pp. 2352-2369.
- Kasischke, E. S., Hyer E. J., Novelli P. C., Bruhwiler L. P., French N. H. F., Sukhinin A. I., Hewson J. H., and Stocks B. J.. 2005. Influences of boreal fire emissions on Northern Hemisphere atmospheric carbon and carbon monoxide, *Global Biogeochem.Cycles*, **19** (GB1012).
- Langenfelds R.L., Francey R.J., Pak B.C., Steele L.P., Lloyd J., Trudinger C.M., and Allison C.E.. 2002. Interannual growth rate variations of atmospheric CO<sub>2</sub> and its  $\delta^{13}\text{C}$ , H<sub>2</sub>, CH<sub>4</sub>, and CO between 1992 and 1999 linked to biomass burning. *Global Biogeochemical Cycles* **16**(3).
- Law K.S. and Nisbet E.G.. 1996. Sensitivity of the CH<sub>4</sub> growth rate to changes in CH<sub>4</sub> emissions from natural gas and coal. *Journal of Geophysical Research* **101**. pp. 14,387-14,397. Cited in Dlugokencky et al. (2001).
- MacDonald J.A., Fowler D., Hargreaves K.J., Skiba U., Leith I.D., and Murray M.B.. 1998. Methane emission rates from a northern wetland; response to temperature, water table and transport. *Atmospheric Environment* **32**. pp. 3219-3227. Cited in Christensen et al. (2003).
- Mastepanov M., Sigsgaard C., Dlugokencky E.J., Houweling S., Ström L., Tamstorf M.P., and Christensen T.R.. 2008. Large tundra methane burst during onset of freezing. *Nature* **456**(7222). pp. 628-630.
- Matthews E. and Fung I.. 1987. Methane emissions from natural wetlands: global distribution, area, and environmental characteristics of sources. *Global Biogeochemical Cycles* **1**(1). pp. 61-86.
- Matthews E., 1989. Global Data Bases on Distribution, Characteristics and Methane Emission of Natural Wetlands: Documentation of Archived Data Tape. NASA TM-4153. National Aeronautics and Space Administration, Washington, D.C..
- Mikaloff Fletcher S.E., Tans P.P., Bruhwiler L.M., Miller J.B., Heimann M.. 2004. CH<sub>4</sub> sources estimated from atmospheric observations of CH<sub>4</sub> and its  $^{13}\text{C}/^{12}\text{C}$  isotop ratios: 1. Inverse modeling of source processes. *Global Biogeochemical Cycles* **18**(GB4004).
- Rigby M., Prinn R.G., Fraser P.J., Simmonds P.G., Langenfelds R.L., Huang J., Cunnold D.M., Steele L.P., Krummel P.B., Weiss R.F., O'Doherty S., Salameh P.K., Wang H.J., Harth C.M., Mühle J., and Porter L.W.. 2008. Renewed growth of atmospheric methane. *Geophysical Research Letters* **35**(L22805).
- Schlesinger, W.H.. 1997. *Biogeochemistry: An Analysis of Global Change*. Academic Press, San Diego, CA. Cited in Chapin III, Matson, and Mooney (2002).
- Simmonds P.G., Manning A.J., Derwent R.G., Ciais P., Ramonet M., Kazan V., Ryall D.. 2005. A burning question. Can recent growth rate anomalies in greenhouse gases be attributed to large-scale biomass burning events?. *Atmospheric Environment* **39**. pp 2513–2517.
- Takeuchi W., Tamura M., and Yasuoki Y., 2003. Estimation of methane emission from West Siberian wetland by scaling technique between NOAA AVHRR and SPOT HRV. *Remote Sensing of Environment* **86**. pp. 21-29.

Van der Werf G.R., Randerson J.T., Collatz G.J., Giglio L., Kasibhatla P.S., Arellano A.F.Jr., Olsen S.C., Kasischke E.S.. 2004. Continental-Scale Partitioning of Fire Emission During the 1997 to 2001 El Niño/La Niña Period. *Science* **303**. pp. 73-76.

Waddington J.M., Roulet N.T., and Swanson R.V.. 1996. Water table control of CH<sub>4</sub> emission enhancement by vascular plants in boreal peatlands. *Geophysical Research Letters* **101**(D17). pp. 22,775-22,785. Cited in Christensen *et al.* (2003).

### *Web sources*

[1] Richter-Menge J., Nghiem S., Perovich D., Rigor I. (?). Arctic report card 2007. Last visited on 10<sup>th</sup> June 2009.

<http://www.arctic.noaa.gov/report07/seaice.html>.

[2] 2007 atmospheric CH<sub>4</sub> growth rate peak. Observations presented at NOAA/ESRL Global Monitoring Division. Last visited 10<sup>th</sup> June 2009.

<http://www.esrl.noaa.gov/gmd/>

[3] *Matthews and Fung* (1987) (see above) wetland data base accessed online at NASA GISS:

<http://data.giss.nasa.gov/landuse/wetland.html>

[4] NCEP/NCAR Reanalysis project gridded temperature data. Accessed online at NOAA/ESRL Physical Science Division:

<http://www.cdc.noaa.gov/data/reanalysis/reanalysis.shtml>

## APPENDIX

---

### Method

**Table I** The temporal resolution of the data variables is defined by these 10 periods. The last four periods are for the purpose of this study defined as autumn.

	Temporal periods	Days
	may.2	16-31 May
	june.1	1-15 June
	june.2	16-30 June
	july.1	1-15 July
	july.2	16-31 July
	aug.1	1-15 Aug.
<b>Autumn</b>	<b>aug.2</b>	<b>16-31 Aug.</b>
	<b>sept.1</b>	<b>1-15 Sept.</b>
	<b>sept.2</b>	<b>16-30 Sept.</b>
	<b>oct.1</b>	<b>1-15 Oct.</b>

The equations for the relevant processing and computation steps in Figure 3.1 are presented below. All presented analysis work was performed in the Matlab computer software.

**Step 2a:** The amount of wetland area in each grid-cell is calculated from the *Matthew and Fung* (1987) data base with *fractional (wetland) inundation*. The two ecosystem types of interest, (1) forested bog and (2) non-forested bog, are extracted as the two data sets are overlaid.

$$\text{Area} = \text{Grid-cell area} * \text{Fractional inundation} \quad (5)$$

*Area* = wetland area in a given grid-cell [m<sup>2</sup>].

*Grid-cell area* = the total surface area [m<sup>2</sup>] within a given grid-cell dependent on the longitudinal and latitudinal cell extent. This area is obtained through a built-in function in the Matlab software.

*Fractional inundation* = the fraction of area within a given grid-cell consisting of wetlands.

**Step 2b:** A linear correlation between variation in air and soil temperature (at 3 cm depth) is assumed, with 0.5 as the slope coefficient. For a fixed grid-cell location and a given period *p* (see Table I):

$$T_A(p) = 0.5 * T_{air}(p) * \text{days}(p) \quad (6)$$

$T_A(p)$  = Accumulated daily soil temperature anomaly [°C day]

$T_{air}(p)$  = Average daily air temperature anomaly [°C]

$\text{days}(p)$  = number of days in period *p* [day]

**Step 3a & b:** To quantify the magnitude of anomalies occurring over wetland area, termed *wetland anomaly*, accumulated temperature anomaly ( $T_A$ ) is multiplied with wetland area (Area). The same calculation is repeated for anomalies over all land surfaces (grid-cell area), giving *land surface anomaly*. For a fixed grid-cell location and a given period  $p$ :

$$A_w(p) = T_A(p) * \text{Area} \quad (7)$$

$$A_L(p) = T_A(p) * \text{grid-cell area} \quad (8)$$

$A_w(p)$  = wetland anomaly [ $^{\circ}\text{C m}^2$ ]

$A_L(p)$  = land surface anomaly [ $^{\circ}\text{C m}^2$ ].

Area = wetland area in a given grid-cell [ $\text{m}^2$ ]; see equation (5)

Grid-cell area = the total surface area [ $\text{m}^2$ ]; see equation (5)

**Step 5a & b:** In the first emission computation approach, for a given period  $p$ , the  $\text{CH}_4$  emission in a grid-cell is computed:

$$\text{Low estimate} \quad \text{CH}_4 = 24 * 0.1702 e^{0.119 T_N(p)} * \text{Area}(p) * T_A(p) \quad (9)$$

$$\text{High estimate} \quad \text{CH}_4 = 24 * 0.2722 e^{0.162 T_N(p)} * \text{Area}(p) * T_A(p) \quad (10)$$

$T_N(p)$  = Normal daily air temperature [ $^{\circ}\text{C}$ ] (see data set in Table 3.1, second row), used as an approximation of normal or “current” soil temperature from which a change (anomaly) in temperature occurs.

Area ( $p$ ) = wetland area in a given grid-cell [ $\text{m}^2$ ]; see equation (5)

$T_A(p)$  = Accumulated daily soil temperature anomaly [ $^{\circ}\text{C day}$ ]; see equation (6). Observe, this variable is half the size of the original *air temperature anomaly* variable ( $T_{\text{air}}$ ), after assumption presented in Section 3.3.

The first part of the equations (9) and (10) are the derivative functions (3) and (4) (see Section 2.4.2) multiplied with 24h in order to make the *anomaly impact* (see definition in Section 3.4) work on a daily basis. Furthermore, *normal daily air temperature* ( $T_N$ ) replaces soil temperature  $T_s$ .

**Step 5c & c:** In the second emission computation approach, normal temperature ( $T_N$ ) is first classified according to the scheme presented in Table 3.2 (see Method).

$$CH_4 = Anomaly\ impact\ (p) * Area\ (p) * T_A\ (p) \quad (11)$$

In this case, *anomaly impact* is predefined for each  $T_N$  class. They are also found in Table 3.2. In this second approach three different settings are furthermore tested for the impact scheme in autumn (defined as the four last periods). These anomaly impacts are displayed in Table II below. Set.1 is the same as the original scheme; Set.2 has amplified anomaly impacts; Set.3 has reduced anomaly impacts.

**Table II** Scheme of *autumn impacts* applied in the three different settings in the second computation approach (see Method). The first settings are unchanged compared to the to the impacts presented in Table 3.2.

Autumn anomaly impact [ $mg\ CH_4\ ^\circ C^{-1}\ m^{-2}\ d^{-1}$ ]						
$T_N$ class	High estimates			Low estimates		
	Set.1	Set.2	Set.3	Set.1	Set.2	Set.3
1	0	0	0	0	0	0
2	24	55	1	11	19	1
3	55	123	24	19	35	11
4	123	231	55	35	56	19
5	231	231	123	56	56	35

Lunds Universitets Naturgeografiska institution. Seminarieuppsatser. Uppsatserna finns tillgängliga på Naturgeografiska institutionens bibliotek, Sölvegatan 12, 223 62 LUND. Serien startade 1985. Uppsatserna är även tillgängliga på <http://www.geobib.lu.se/>

The reports are available at the Geo-Library, Department of Physical Geography, University of Lund, Sölvegatan 12, S-223 62 Lund, Sweden.  
Report series started 1985. Also available at <http://www.geobib.lu.se/>

111. Tränk, L., (2005): Kadmium i skånska vattendrag – en metodstudie i föroreningsmodellering.
112. Nilsson, E., Svensson, A.-K., (2005): Agro-Ecological Assessment of Phonxay District, Luang Phrabang Province, Lao PDR. A Minor Field Study.
113. Svensson, S., (2005): Snowcover dynamics and plant phenology extraction using digital camera images and its relation to CO<sub>2</sub> fluxes at Stordalen mire, Northern Sweden.
114. Barth, P. von., (2005): Småvatten då och nu. En förändringsstudie av småvatten och deras kväveretentionsförmåga.
115. Areskoug, M., (2005): Planering av dagsutflykter på Island med nätverkanalys
116. Lund, M., (2005): Winter dynamics of the greenhouse gas exchange in a natural bog.
117. Persson, E., (2005): Effect of leaf optical properties on remote sensing of leaf area index in deciduous forest.
118. Mjöfors, K., (2005): How does elevated atmospheric CO<sub>2</sub> concentration affect vegetation productivity?
119. Tollebäck, E., (2005): Modellering av kväveavskiljningen under fyra år i en anlagd våtmark på Lilla Böslid, Halland
120. Isacson, C., (2005): Empiriska samband mellan fältdata och satellitdata – för olika bokskogområden i södra Sverige.
121. Bergström, D., Malmros, C., (2005): Finding potential sites for small-scale Hydro Power in Uganda: a step to assist the rural electrification by the use of GIS
122. Magnusson, A., (2005): Kartering av skogsskador hos bok och ek i södra Sverige med hjälp av satellitdata.
123. Levallius, J., (2005): Green roofs on municipal buildings in Lund – Modeling potential environmental benefits.
124. Florén, K., Olsson, M., (2006): Glacifluviala avlagrings- och erosionsformer I sydöstra Skåne – en sedimentologisk och geomorfologisk undersökning.
125. Liljewalch-Fogelmark, K., (2006): Tågbuller i Skåne – befolkningens exponering.
126. Irminger Street, T., (2006): The effects of landscape configuration on species richness and diversity in semi-natural grasslands on Öland – a preliminary study.
127. Karlberg, H., (2006): Vegetationsinventering med rumsligt högupplösande satellitdata – en studie av QuickBird-data för kartläggning av gräsmark och konnektivitet i landskapet.
128. Malmgren, A., (2006): Stormskador. En fjärranalytisk studie av stormen Gudruns skogsskador och dess orsaker.
129. Olofsson, J., (2006): Effects of human land-use on the global carbon cycle during the last 6000 years.

- 130 Johansson, T., (2006): Uppskattning av nettoprimärproduktionen (NPP) i stormfällan efter stormen Gudrun med hjälp av satellitdata.
- 131 Eckeskog, M., (2006): Spatial distribution of hydraulic conductivity in the Rio Sucio drainage basin, Nicaragua.
- 132 Lagerstedt, J., (2006): The effects of managed ruminants grazing on the global carbon cycle and greenhouse gas forcing.
- 133 Persson, P., (2007): Investigating the Impact of Ground Reflectance on Satellite Estimates of Forest Leaf Area Index
- 134 Valoczi, P. (2007): Koldioxidbalans och koldioxidinnehållsimulering av barrskog i Kristianstads län, samt klimatförändringens inverkan på skogen.
- 135 Johansson, H. (2007): Dalby Söderskog - en studie av trädarternas sammansättning 1921 jämfört med 2005
- 137 Kalén, V. (2007): Analysing temporal and spatial variations in DOC concentrations in Scanian lakes and streams, using GIS and Remote Sensing
- 138 Maichel, V. (2007): Kvalitetsbedömning av kväveretentionen i nyanlagda våtmarker i Skåne
- 139 Agardh, M. (2007): Koldioxidbudget för Högestad – utsläpp/upptag och åtgärdsförslag
- 140 Peterz, S. (2007): Do landscape properties influence the migration of Ospreys?
- 141 Hendrikson, K. (2007): Småvatten och groddjur i Täby kommun
- 142 Carlsson, A. (2008): Antropogen påverkan i Sahel – påverkar människans aktivitet NDVI uppmätt med satellit.
- 143 Paulsson, R. (2008): Analysing climate effect of agriculture and forestry in southern Sweden at Högestad & Christinehof Estate
- 144 Ahlstrom, A. (2008): Accessibility, Poverty and Land Cover in Hambantota District, Sri Lanka. Incorporating local knowledge into a GIS based accessibility model.
- 145 Svensson T. (2008): Increasing ground temperatures at Abisko in Subarctic Sweden 1956-2006
- 146 af Wåhlberg, O. (2008): Tillämpning av GIS inom planering och naturvård - En metodstudie i Malmö kommun.
- 147 Eriksson, E. och Mattisson, K. (2008): Metod för vindkraftslokalisering med hjälp av GIS och oskarp logik.
- 148 Thorstensson, Helen (2008): Effekterna av ett varmare klimat på fenologin hos växter och djur i Europa sedan 1950.
- 149 Raguz, Veronika (2008): Karst and Waters in it – A Literature Study on Karst in General and on Problems and Possibilities of Water Management in Karst in Particular.
- 150 Karlsson, Peggy (2008): Klimatförändringarnas inverkan på de svenska vägarna.
- 151 Lyshede, Bjarne Munk (2008): Rapeseed Biodiesel and Climate Change Mitigation in the EU.
- 152 Sandell, Johan (2008): Detecting land cover change in Hambantota district, Sri Lanka, using remote sensing & GIS.
- 153 Elgh Dalgren, Sanna (2008): vattennivåförändringar i Väneren och dess inverkan på samhällsbyggnaden i utsatta städer
- 154 Karlgård, Julia (2008): Degradation of peat mires in northern Europe: changing vegetation in an altering climate and its potential impact on greenhouse gas fluxes.
- 155 Dubber, Wilhelm and Hedbom, Mari (2008) Soil erosion in northern Loa PDR

- An evaluation of the RUSLE erosion model
- 156 Cederlund, Emma (2009): Metodgranskning av Klimatkommunernas lathund för inventering av växthusgasutsläpp från en kommun
- 157 Öberg, Hanna (2009): GIS-användning i katastrofdrabbade utvecklingsländer
- 158 Marion Früchtl & Miriam Hurkuck (2009): Reproduction of methane emissions from terrestrial plants under aerobic conditions
- 159 Florian Sallaba (2009): Potential of a Post-Classification Change Detection Analysis to Identify Land Use and Land Cover Changes. A Case Study in Northern Greece
- 160 Sara Odelius (2009): Analys av stadsluftens kvalitet med hjälp av geografiska informationssystem.
- 161 Carl Bergman (2009): En undersökning av samband mellan förändringar i fenologi och temperatur 1982-2005 med hjälp av GIMMS datasetet och klimatdata från SMHI.
- 162 Per Ola Olsson (2009): Digitala höjdm modeller och höjdsystem. Insamling av höjddata med fokus på flygburen laserskanning.
- 163 Johanna Engström (2009): Landskapets påverkan på vinden - sett ur ett vindkraftperspektiv.
- 164 Andrea Johansson (2009): Olika våtmarkstypers påverkan på CH<sub>4</sub>, N<sub>2</sub>O och CO<sub>2</sub> utsläpp, och upptag av N<sub>2</sub>.
- 165 Linn Elmlund (2009): The Threat of Climate Change to Coral Reefs
- 166 Hanna Forssman (2009): Avsmältningen av isen på Arktis - mätmetoder, orsaker och effekter.
- 167 Julia Olsson (2009): Alpina trädgränsens förändring i Jämtlands- och Dalarnas län över 100 år.
- 168 Helen Thorstensson (2009): Relating soil properties to biomass consumption and land management in semiarid Sudan – A Minor Field Study in North Kordofan
- 169 Nina Cerić och Sanna Elgh Dalgren (2009): Kustöversvämningar och GIS - en studie om Skånska kustnära kommuners arbete samt interpolationsmetodens betydelse av höjddata vid översvämningssimulering.
- 170 Mats Carlsson (2009): Aerosolers påverkan på klimatet.
- 171 Elise Palm (2009): Övervakning av gåsbete av vass – en metodutveckling. Delprojekt i miljöeffektuppföljningen av Vänerns nya vattenreglering.
- 172 Sophie Rychlik (2009): Relating interannual variability of atmospheric CH<sub>4</sub> growth rate to large-scale CH<sub>4</sub> emissions from northern wetlands